2014

Determining How Defects in Connexin 43 Cause Skeletal Diseases

Quynh V. Ton
Lehigh University

Determining How Defects in Connexin 43 Cause Skeletal Diseases

by

Quynh V. Ton

A Dissertation

Presented to the Graduate and Research Committee

of Lehigh University

in Candidacy for the Degree of

Doctor of Philosophy

in

Molecular Biology

Lehigh University

January 2014

Approved and recommended for acceptance as a dissertation in partial fulfillment of the requirements for the degree of Doctor of Philosophy

Quynh V. Ton
Determining How Defects in Connexin 43 Cause Skeletal Diseases

_____

Defense Date

_____

Dissertation Director
M. Kathryn Iovine, PhD

_____

Approved Date

Committee Members:

_____

Matthias M. Falk, PhD

_____

Michael Kuchka, PhD

_____

Linda Lowe-Krentz, PhD

_____

Kenneth Poss, PhD

ACKNOWLEDGMENTS

I wish first to express my sincere appreciation to Dr. Kathy Iovine, my graduate mentor. Your advice, guidance, understanding and constant support have shaped my graduate career to success. Thank you so much for being with me when I thought I could have failed the program. Thank you for thinking ahead and helping me to find the solution for the problems. Your expectations and high standards ultimately helped me to improve and develop into a form of scientist I am today. I will miss working with you….will miss hours of making figures on photoshop….hours of writing manuscripts….hours of making presentations that later I know you would ask me to correct them all over again but I know in the end they would look/sound good, clean and pretty.

To my mother and father, the first and forever teachers of my life. I have no words to describe how much I thank you for what you had sacrificed for me so that I could have a better life and better education. Dad, you were with me 24/7 taking care of my sickness when I was a little child. You taught me from how to make the first baby step to how to do math and later how to become a good person that carries a warm heart and dignity. Your lessons will always be with me…will help me continue to stand strong when I face challenges in life. Though you are no longer here with me, I know in the end we will meet and will together once again continue the daughter-father journey… Mom, your strict teaching helped me to become a strong and determined woman. I truly hope you will live long with us to see your first future grand-children…to help me teach them just like the way you did to me so that they can also become strong and independent.

To my wonderful thesis committee members, without your critics and encouragements, I never would have accomplished this. To Dr. Poss, thank you so much for taking your time to give me valuable inputs. Thank you for pushing me forward, for making me to think harder in each scientific scenario. Your suggestions have helped me to see the

whole aspects of my research, to find the way to apply what I have learned to solve the problem.

To professors and entire staff in the Biology Department, thank you so much for your extensive help and administrative/technical support. Dr. Kuchka, Dr. Lowe-Krentz, Dr. Skibben, and Dr. Cassimeris, thank you for your wonderful teachings. I learned so much from your classes, I feel well-rounded and I am certain that whatever I learn from your classes will eventually help my career. To Dr. Cassimeris and Dr. Falk, thank you so much for taking your time to write letters of recommendation. I would not have had a post doctoral position if I did not get good words from you.

Finally, my most gratitude must go to my wonderful family. To Chris, I know you are trying to understand my career and several times you keep asking me how long this process can take me to cure the world… to become an awesome scientist. Your supports and patience have meant lots to me though many times I did not show it to you enough. Thank you for hours of driving me to feed and help to feed the fish….hours of comforting when my experiments did not work ….hours of trying to soothe my anxiety.

To Karen and Fred, my second parents, I cannot thank you enough for your constant supports….being there when things turn either ups or downs….assuring me that everything will be fine because I am the best and no one can replace me.

To the Iovine lab and all my good friends, you guys are so awesome. Your friendship helps me believe that indeed true friends exist. Wuti, John and Som, my good friends, my colleagues, you guys helped me a lot during the qualifying exam. Without hours that you spent to quiz me, I would not have passed the test.

Last but not least, to people that have helped me along the way, since the day I put my foot in the US to the day I entered college then graduate program. I remember and will remember how much you have done for me and how much you have made my life from

impossible to possible. Words are not enough to express my appreciation for that…

TABLE OF CONTENTS

LIST OF FIGURES AND TABLES

LIST OF ABBREVIATIONS

µg	Microgram
µL	Microliter
µm	Micrometer
µM	Micromolar
another long fin	*alf* ^{dty86}
collagen	*col*
cRNA	Complementary RNA
Cx	Connexin
dpa	Day post amputation
dpe	Day post electroporation
EDTA	Ethylenediaminetetraacetic acid
even skipped	*evx*
FGF	Fibroblast growth factor
GJIC	Gap junctional intercellular communication
hpa	Hour post amputation
HYB	Hybridization solution
Hpa	Hour post amputation
KD	Knockdown
kDa	Kilodalton
MABT	Maleic acid buffer with tween 20 solution
matrix metallopeptidase	*mmp*
distal-less homeobox	*dlx*

miRNA	Micro RNA
MO	Morpholino
mRNA	Messenger ribonucleic acid
NBT/BCIP	nitro-blue tetrazolium/5-bromo-4-chloro-3'- indolyphosphate
neuropillin	*nrp*
PBS	Phosphate buffered saline
PBST	Phosphate buffered tween 20 saline
PCR	Polymerase chain reaction
plexin	*plx*
qRT-PCR	Quantitative real time polymerase chain reaction
RNA	Ribonucleic acid
rRNA	Ribosomal RNA
semaphorin	*sema*
shh	*sonic hedegehog*
short fin	*sof* ^{b123}
SSC	Saline sodium citrate solution
tRNA	Transfer RNA

Abstract

The zebrafish fin is composed of multiple bony fin rays. Each fin ray is comprised of multiple segments separated by joints. Regulatory mechanisms that control joint morphogenesis and ray segment length in zebrafish fins are not fully understood. We utilize the fin length mutants *short fin* (*sof* ^{b123}) and *another long fin* (*alf* ^{dty86}) to provide insight into these processes. The *sof* ^{b123} mutant has short fins and short segments due to a mutation in the gap junction protein gene *connexin43* (*cx43*). In contrast, the *alf* ^{dty86} mutant has long fins, long segments, and over-expression of *cx43*. Thus, the two mutants exhibit two opposing phenotypes. For example, the *sof* ^{b123} mutant exhibits reduced *cx43* mRNA and the *alf* ^{dty86} mutant exhibits increased *cx43* mRNA. Cx43 knockdown in *alf* ^{dty86} rescues the segment length phenotype suggesting that Cx43 activity regulates joint formation. These data suggest that Cx43 is involved in two independent pathways: promoting cell division and suppressing joint formation. This thesis dissertation is a collection of my entire graduate work mainly focused on Cx43-dependent events that coordinate cell proliferation and joint formation. Identification of genes acting downstream of *cx43* revealed *semaphorin3d* (*sema3d*). Sema3d is a secreted ligand and is known to play various roles including axon guidance, vasculature patterning and cell proliferation. Here I found *sema3d* is functionally downstream of *cx43* and mediates *cx43*-dependent pathways. Moreover, independent receptors of Sema3d were identified that may regulate cell proliferation and joint formation in zebrafish fin regeneration. I provide evidence that through Sema3d, Cx43 regulates an

evx1-dependent joint pathway to suppress joint differentiation. Additional data show that to permit the joint pathway, *cx43* mRNA is transiently reduced. Continued studies on joint morphology and gene expression in the *sof* and *alf* mutants as well as characterization of the Cx43 protein will provide evidence whether Cx43 indeed regulates joint development. These future findings will ultimately provide us with keen insights into roles of Cx43 that are reflected via a specific time line of gene expression.

CHAPTER 1

INTRODUCTION

1.1 Regeneration background and history

One of the features of most multicellular organisms is that they have the capacity to maintain their tissue integrity by either regenerating a new form or by replacing the lost or damaged tissue for a new tissue. For such processes, it is likely that multiple growth control mechanisms as well as cell proliferation and other cellular signaling pathways are required. However, the regulative processes of regeneration are far from being understood. It is interesting that some lower vertebrates have a major ability to maintain their bodies by which they reform and regenerate their body parts such as limbs and tails. Mammals such as human maintain the body architecture through the process of wound healing but largely cannot regenerate lost or damaged body parts.

Humans have been aware of such differences in the regeneration capacities between mammals and lower vertebrates since ancient times. An example of this awareness is the story of Prometheus and his liver regeneration. Prometheus is known as an ancient Greek, a hero for humankind. He was punished by Zeus for stealing the secret of fire. Prometheus thus was chained and tormented by an eagle. The eagle preyed on his liver, which was regenerated as fast as it was devoured. However, it was not until 18th century when regeneration became more appreciated. The first scientist who made a major contribution in the regeneration field is Abraham Trembley. He discovered one of the first regenerative species Hydra in 1744 (Dinsmore, 1991). Followed shortly after his discovery, several scientists began to identify other species (i.e. salamander, newt) that have capability to regenerate their own lost body parts.

Currently, regenerative medicine is a relatively young field where our findings on regeneration (i.e. pluripotent stem cells or scaffolds for tissue repair) may be applied to benefit human health. Researchers have tried to understand how the process occurs in the regenerative species. Still, they have not fully understood the differences in the capacities between regenerative and non-regenerative animals. They speculate that such differences in the capacities are due to gene loss during evolution or due to different enzymes or proteins that play an important role in tissue maintenance and tissue homeostasis (Ishida et al., 2010). Others hypothesize that regulatory genes required for regeneration become silenced in the organisms that have no regeneration capacity. For example, histone modifications may be necessary for regeneration activation (Stewart et al., 2009). Demethylation that causes the loss of histone function is activated during fin regeneration (Stewart et al., 2009). However, it is unclear what and how signals generated to regulate the demethylation process once the fin gets amputated. Thus, it is important to understand the fundamental mechanism at the molecular, cellular and genetic levels underlying tissue morphogenesis to answer the question why higher vertebrates have less opportunity to regenerate than lower vertebrates. Once the answer is found, we could have a better understanding about regeneration and could apply the knowledge to seek better treatment for many diseases and injuries that cause tissue damage or organ failure in order to improve the quality of human life.

1.2 Zebrafish caudal fins provide advantages for studies in skeletogenesis

For a decade, researchers have utilized zebrafish to study regeneration (reviewed in Kawakami, 2010). The zebrafish has the capacity to regenerate several organs

including retina, spinal cord and fin. The zebrafish fins are easily accessible mostly at every stage of development (from larvae to adult). The fin grows throughout its lifetime, is able to re-grow rapidly after being amputated, and is not required for viability. Thus, it is convenient for us to evaluate changes in cell proliferation and gene expression throughout the regeneration stages. Further, methods of targeted gene knockdown using anti-sense morpholino oligos have been successfully established in the regenerating fins (Thummel et al., 2006). Thus, several laboratories have routinely applied these methods to identify phenotypic effects due to changes in gene expression.

The zebrafish fin also offers several advantages to the study of bone growth. The fin itself is comprised of an endoskeleton (inside the body wall) and an exoskeleton comprised of multiple segmented fin rays, where each segment is flanked by osteoblast-free-regions (or fin ray joints or simply joints) (reviewed in Iovine 2007). Each fin ray is formed of two hemirays of bone matrix surrounding a mesenchyme of undifferentiated cells as well as vasculature and neurons. Each hemiray at the distal end includes actinotrichia, which serves as a substrate for osteoblasts to align and secrete bone matrix (Becerra et al., 1983). Thus, osteoblasts are found laterally in association with the bone matrix, while the mesenchyme is located medially. During normal growth, differentiated osteoblasts never or rarely divide (Johnson and Bennett 1999). Moreover, fin grows in the proximal to distal direction and new segments and joints are continually added to the distal end of the fin ray. Once established, segments do not increase in length but rays increase in diameter (Iovine and Johnson, 2000; Sims et al., 2009) (Figure 1.1). Thus, the length of fin ray is maintained a constant proportion to the fish body. This constant

proportion is strictly followed even when the rate of growth slows down as fish matures, suggesting that growth is isometric growth with respect to body growth (Iovine and Johnson 2000).

Following amputation, fin regenerates rapidly in proximal-distal direction and ceases approximately after one month when fin size and tissue pattern are restored. In addition, differentiated osteoblasts near the amputation plane become highly active (Johnson and Bennett 1999). Repeated amputation does not affect the regenerative capacity (Azevedo et al., 2011). Fin regeneration has been found to proceed through several discrete stages: (i) wound healing; (ii) blastema formation; and (iii) the fin ray formation/distal outgrowth (Akimenko et al., 2003; Poss et al., 2003; Figure 1.2). After amputation, the tissue initiates the wound healing process. Blood from the injured capillaries accumulates at the wound, to form a temporary closure called apical epithelial cap (AEC) (Becerra et al., 1996). Recent studies show that the cells of a different linage from the stump respond to the injury via dedifferention into a precursor cell type population. They proliferate and accumulate underneath the wound epithelium to form a blastema where later, under appropriate signals, these cells will re-differentiate into different cell types (Knopf et al., 2011; Singh et al., 2012; Sousa et al., 2011; Tu and Johnson 2011). Cells in the blastema are divided into two groups: the distal most blastema that is known to be slowly cycling (or none), and a large population of highly proliferative cells (Nechiporuk and Keating, 2002; Poss et al., 2002). It has been known that the wound epidermis is required for the initiation of regeneration. Without the apical wound epidermis, regeneration is terminated (reviewed in Kawakami, 2010). Wound

healing and the establishment of wound epidermis require FGF and Wnt/β-catenin (reviewed in Stoick-Cooper et al., 2007). Likewise, FGF and Wnt/β-catenin signaling pathways are essential for blastema formation and the outgrowth process (reviewed in Stoick-Cooper et al., 2007). Moreover, a recent study shows that reactive oxygen species (ROS) specifically hydrogen peroxide (H_2O_2) play a critical role for blastema formation during the first 24 hpa (Gauron et al., 2013).

Outgrowth follows and proceeds approximately 2-4 weeks. During the outgrowth stages, cells of the proximal blastema divide rapidly, move in the proximal direction to differentiate, replacing the lost tissue. One possibility is that the zone of negative proliferation in the distal-most blastema maintains directionality of the outgrowth to the cells of the proximal blastema. The basal layer of epidermis (i.e. the cell layer of the epidermis closest to the mesenchymal compartment) also appears to provide growth and patterning cues to the underlying mesenchyme (reviewed in Iovine, 2007). For example, *sonic hedegehog* (*shh*) is detected in a subset of cells in the lateral basal layer of the epidermis, where its expression has been suggested to determine some aspects of skeletal differentiation and patterning underlying the differentiating osteoblasts (Avaron et al., 2000). Another example is *bone morphogenetic protein 2b* (*bmp2b*), expressed in the distal basal epidermal layer in a pattern similar to that of *shh*, as well as in the osteoblasts (Avaron et al., 2000). Wnt5b acts as a negative regulator during fin outgrowth (reviewed in Stoick-Copper et al., 2013). Recent studies show that osteoblasts and joint forming cells appear to be derived from a common lineage (Tu and Johnson 2011). When these cells start to re-differentiate, osteoblasts express their transcription factors (*runx2a*,

runx2b, and *osx*) (Brown et al., 2009), while joint forming cells express their transcription factor such as *evx1*. Thus, we refer to cells in the distal-lateral mesenchyme collectively as "skeletal precursor cells."

1.3 Cx43 function is conserved during skeletal morphogenesis

Our lab is interested in the study of skeletal morphogenesis underlying regulation of growth and joint development during zebrafish fin regeneration. We took a genetic approach to identify genes contributing to skeletal morphogenesis by evaluating the recessive *short fin* (*sof*^{b123}) mutant. The *sof*^{b123} mutant exhibits short fin length, short segment length, reduced cell proliferation, and is caused by a mutation in *connexin43* (*cx43*) (Iovine et al., 2005) (Figure 1.3). Due to the mutation, the *sof*^{b123} mutant also exhibits reduced *cx43* mRNA and protein without a lesion in the coding sequence (Hoptak-Solga et al., 2008; Iovine et al., 2005). In addition to *sof*^{b123}, three additional alleles (*sof*^{j7e1}, *sof*^{j7e2}, and *sof*^{j7e3}) that were identified by non-complementation screen assay have reduced GJIC activity (Hoptak-Solga et al., 2007). Importantly, morpholino-mediated targeted gene knockdown of *cx43* (i.e. causing reduced Cx43 protein) causes reduced fin length, reduced segment length and reduced cell proliferation, completely recapitulating the *short fin* phenotypes (Hoptak-Solga et al., 2008). Thus, any loss of Cx43 function (reduced mRNA, protein or GJIC) lead to the same set of phenotypes: reduced fin length, reduced segment length and reduced cell proliferation.

Connexins are the subunits of gap junction channels that are believed to play a role in direct cell-cell communication of ions and metabolites that are ≤1200 Da. Each connexin is a four pass transmembrane spanning domain protein. Six of them oligomerize

to form a hemichannel called a connexon. One connexon at the plasma membrane will pair with another connexon from the adjacent to form a complete gap junction channel (Figure 1.4). Defective Cx43 function causes skeletal defects in human, mouse, chick, and zebrafish. Missense mutations in human *CX43* result in an autosomal dominant disorder called oculodentodigital dysplasia (ODDD, Paznekas et al., 2003). Patients with ODDD exhibit major skeletal malformations and craniofacial abnormalities such as cranial hyperostosis and broad tubular bones. This disease has additional pleiotropic phenotypes including eye abnormalities leading to vision loss and dental anomalies (reviewed in Pfenniger et al., 2010). The range of phenotypes affecting multiple tissues is likely due to the fact that *CX43* is expressed in most cell types. Similarly, the $Gja1^{jrt/+}$ mouse carries a mutation coding for a dominant missense mutation in the *CX43* gene, and exhibits skeletal and pleiotropic phenotypes similar to those observed in human ODDD (Flenniken et al., 2005). Indeed, recently generated knock-in alleles, where human Cx43-missense mutations replace the endogenous wild-type Cx43 allele in the mouse, also mimic human ODDD (Dobrowolski et al., 2008; Watkins et al., 2011). In contrast, the *CX43* knockout mouse ($CX43^{-/-}$) dies prenatally due to defects in the heart outflow tract and reduced blood flow to tissues (Reaume et al., 1995). Continued investigation revealed that these mice exhibit delayed ossification of both the intramembranous and endochondral skeletons (Lecanda et al., 2000). To further overcome the lethality of $CX43^{-/-}$, conditional *CX43* knockout mouse lines have been generated. While mice lacking Cx43 activity in osteoblasts are viable, they exhibit reduced bone mineral density throughout their skeletons, consistent with phenotypes observed in the complete

knockout (Chung et al., 2006; Watkins et al., 2011; Zhang et al., 2012; Bivi et al., 2012). Targeted gene knockdown of *CX43* in adult chicks and in chick embryos results in facial defects and limb malformation, respectively (Makarenkova et al., 1999; McGonnell et al., 2001). Finally, in the zebrafish, homozygous mutations in the *cx43* gene cause the *short fin* (*sof*^{b123}) phenotype which primarily affects the fin skeleton. In addition, targeted gene knockdown of *cx43* causes embryonic heart defects, suggesting *cx43* is essential (Iovine et al., 2005). Collectively, these data demonstrate that Cx43 function is conserved from fish to man and is required for typical skeletal morphogenesis in vertebrates.

1.4 Cx43 regulates two independent pathways in vivo

Previous studies in the *sof* mutant from our lab suggest the likelihood of direct cell-cell communication from Cx43-dependent GJIC is required for growth of the boney fin ray segments. Prior work from our lab demonstrated that the three missense alleles of *cx43* exhibit reduced levels of GJIC in heterologous assays (these alleles also appear to be capable of trafficking to the plasma membrane, Hoptak-Solga et al., 2007). Further, the severity of the segment length and cell proliferation phenotypes is correlated with the reduced level of GJIC (Iovine et al., 2005; Hoptak-Solga et al., 2008), strongly suggesting that reduced Cx43-based GJIC is responsible for the observed skeletal defects. In addition, we found *another long fin* (*alf*^{dty86}, van Eeden et al., 1996) mutant exhibits over-expression of *cx43* mRNA. This mutant is known for long fins with irregular joint formation (Figure 1.3). Indeed, *cx43* knockdown in *alf*^{dty86} rescues irregular segment length (Sims et al., 2009), suggesting that the joint failure phenotype is the result of increased expression of *cx43*. Since the *alf*^{dty86} mutant exhibits phenotypes opposite to

that of *sof*, and as *cx43* knockdown rescues those phenotypes, we consider *alf* ^{dty86} to be a mimic of *cx43* over-expression but we do know that the best way to utilize over-expression phenotypes is to make a *cx43* over-expression transgenic line.

One could speculate that reduced cell proliferation of *sof* leads directly to its observed reduced segment length. However, manipulation of growth rate is not sufficient to alter segment length (Iovine and Johnson, 2000). Segment length is the same in similarly sized fins, regardless of their growth rate, suggesting that the rate of cell proliferation does not determine segment length. Further, changing cell proliferation is not sufficient to alter segment length. For example, inhibition of cell proliferation such as blocking Fgfr1 or Shh signaling pathways does affect fin growth but does not alter segment length (Lee et al., 2005; Quint et al., 2002). Together these findings suggest that segment length is a reflection of joint placement. Further, we propose that Cx43 has two activities: it promotes cell proliferation and suppresses joint formation.

1.5 Hypotheses and Research Objectives

Findings from the Iovine lab have suggested that Cx43 coordinates cell proliferation and joint formation to precisely regulate fin growth and segment length. Little is known mechanistically regarding how Cx43 regulates such events. Thus, the goal of my research was to identify the tangible events regulated by GJIC, specifically on the role of Cx43 in zebrafish.

1) One hypothesis is that Cx43-based GJIC influences gene expression (Stains et al., 2003). To identify global changes in gene expression occurring downstream of *cx43*, the Iovine lab utilized a microarray strategy, focusing on the subset of genes both

down-regulated in *sof* ^{b123} and up-regulated in *alf* ^{dty86} to enable the identification of *cx43*-dependent genes. To date, there are 15 genes that are validated to have *cx43* dependent functions. Among the 15 genes, I am interested in *semaphorin3d* (*sema3d*) since it is a secreted ligand which has a promising potential to provide insights into how Cx43 mediates cell proliferation and joint formation. Sema3d belongs to a Semaphorin family that first identified as guidance cues for axons (Kolodkin et al., 1992). More recently, roles of Semas have been discovered to play roles in cell proliferation, tissue pattering, cancer, immunity, and bone protection (reviewed in Roth et al., 2009). Class 3 Semas including Sema3d utilize transmembrane receptors Neuropilin (Nrps) and Plexins (Plxns) to transduce signals into the cell. Studies show that in some instances, Semas can provide different outcomes if they bind either Nrps or Plxns or both (Wolman et al., 2004). It is interesting that *sema3d* is expressed in regenerating fins since there is no study reported any role of *sema3d* in fin regeneration. Thus, the identity of Sema3d, its receptors, and its downstream events need to be determined. This objective is presented as Chapter 2. I discovered that Sema3d utilizes Nrp2a and PlxA3 to mediate Cx43 dependent skeletal and patterning phenotypes (Ton and Iovine, 2012).

2) Both *cx43* mRNA and Cx43 protein are expressed throughout the medial mesenchyme, concentrated mostly in the blastema (Figure 1.5). This population is adjacent to the lateral populations of skeletal precursor cells. I hypothesize that there is communication between the medial *cx43*-positive mesenchyme and the lateral mesenchymal compartment. Previously, the Iovine lab showed that Cx43 suppresses

joint formation. Further, results from our lab show that cells expressing early genes for osteoblasts and joint-forming cells are located directly adjacent to the *cx43*-positive mesenchymal cells (Brown et al., 2009). It is possible that Cx43 suppresses joint differentiation by either suppressing a joint pathway and/or promoting an osteoblast pathway. Thus, a joint pathway/an osteoblast pathway that works downstream of *cx43* needs to be defined and which pathway that Cx43 would favor needs to be determined. This objective is represented as Chapter 3. I discovered that there is an *evx1*-dependent joint pathway that is regulated by Cx43 activity which suggests that Cx43 may regulate joint formation by influencing the timing of *evx1* expression (Ton and Iovine, in revision).

3) It is unclear how Cx43 activity is regulated to contribute to growth and patterning. One possibility is that *cx43* levels fluctuate over time. As a starting point, I chose to evaluate *cx43* mRNA levels in concert with the initiation of new fin regenerating joints during regeneration. I notice that *cx43* gene expression is transiently reduced when a new joint is initiated. In addition, Cx43 regulates joint formation by utilizing Sema3d signaling pathway which coordinates with gene expression in the *evx1*-dependent joint pathway. However, it is unclear how Cx43-dependent GJIC in the blastemal cells influences *sema3d* gene expression in the adjacent skeletal precursor cells, thereby suppressing joint gene expression. These objectives are represented as Chapter 4 under the "remaining questions" section. Chapter 4 also highlights future directions in an attempt to reveal the initial Cx43-dependent event that regulates

changes in cellular function. Most of the highlights belong to the unpublished work and the published review paper: Ton and Iovine, 2013.

1.6 Figures

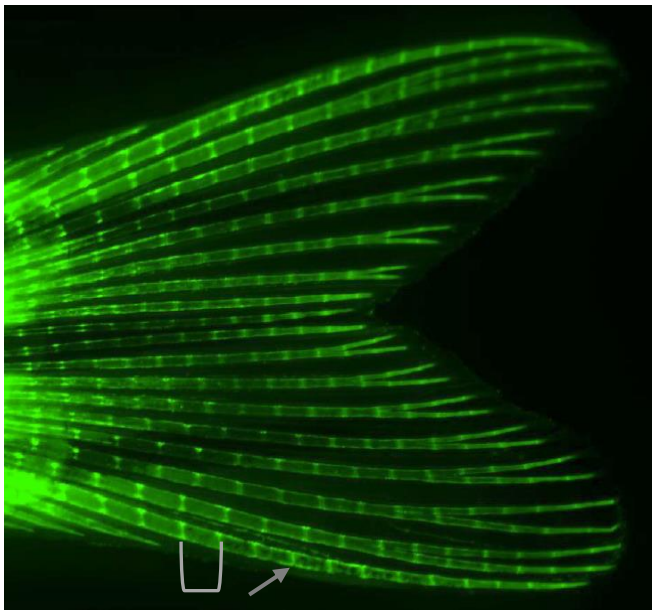

Figure 1.1: The zebrafish fin is a model system for skeletal morphogenesis. The caudal fin is stained with calcein (detects bone matrix) revealing fin rays containing bony segments (bracket) separated by joints (arrow).

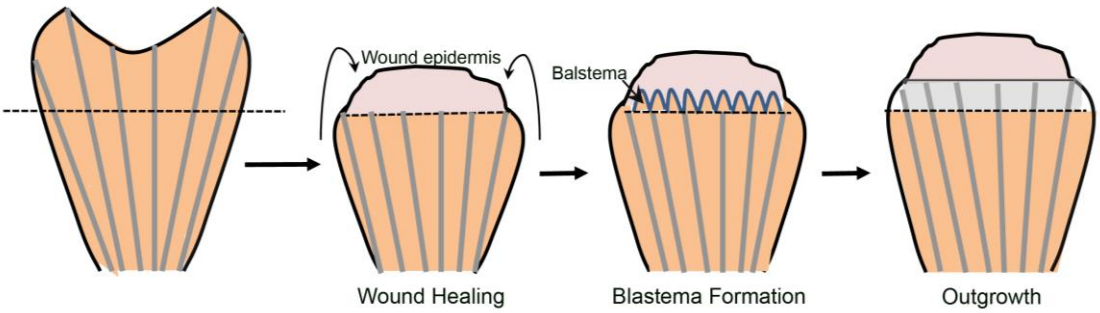

Figure 1.2: Fin regeneration stages. Wound healing, blastema formation and outgrowth. During wound healing, epithelial cells migrate distally to cover the wound by forming an apical epithelial cap (AEC). Cells in the blastema are divided into two subsets: distal most blastema that has slow cycling cells and cells that are highly proliferative.

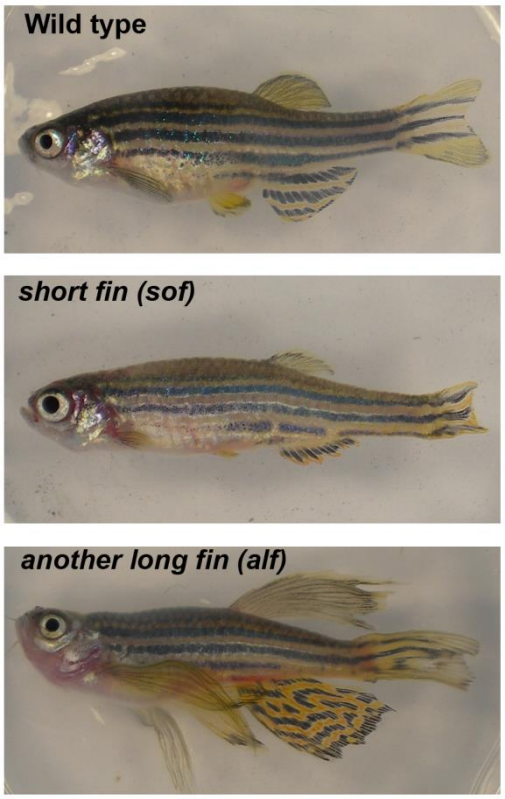

Figure 1.3: Fin length mutants exhibit defects in skeletal morphogenesis. Top: wild-type zebrafish. Middle: *sof* ^{b123} mutant. Bottom: *alf* ^{dty86} mutant. (Reviewed in Ton and Iovine, 2013).

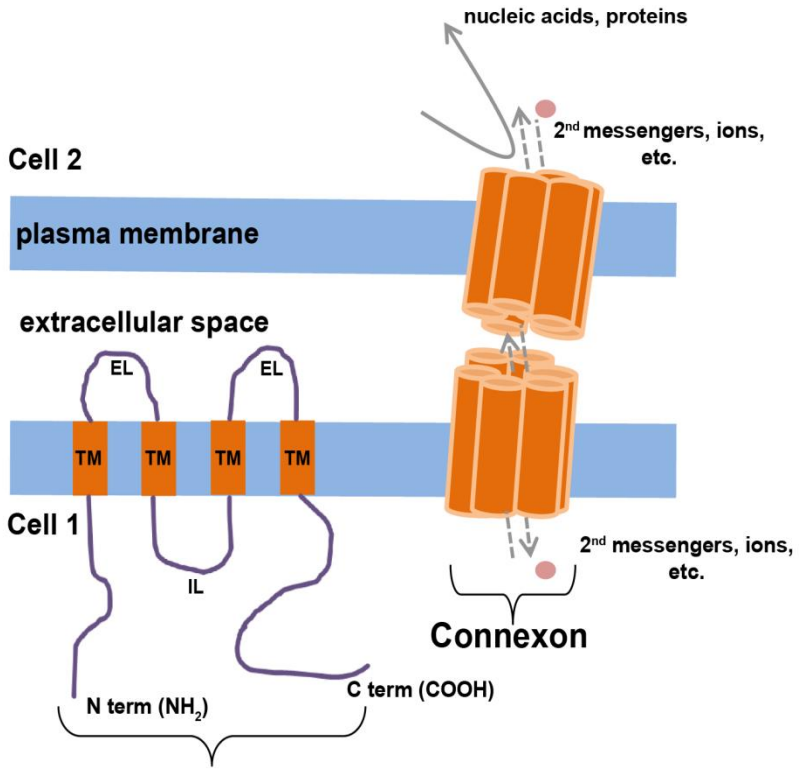

Figure 1.4: Gap junction channels connect the cytoplasm of adjacent cells. Each connexin contains four transmembrane-spanning domains, with both the amino and carboxy ends located in the cytoplasm. Six connexins comprise a connexon, or hemichannel. Two connexons, one from each cell, dock together at the plasma membrane to make a single gap junction channel. IL, intracellular loop; EL, extracellular loop. (Reviewed in Ton and Iovine, 2013).

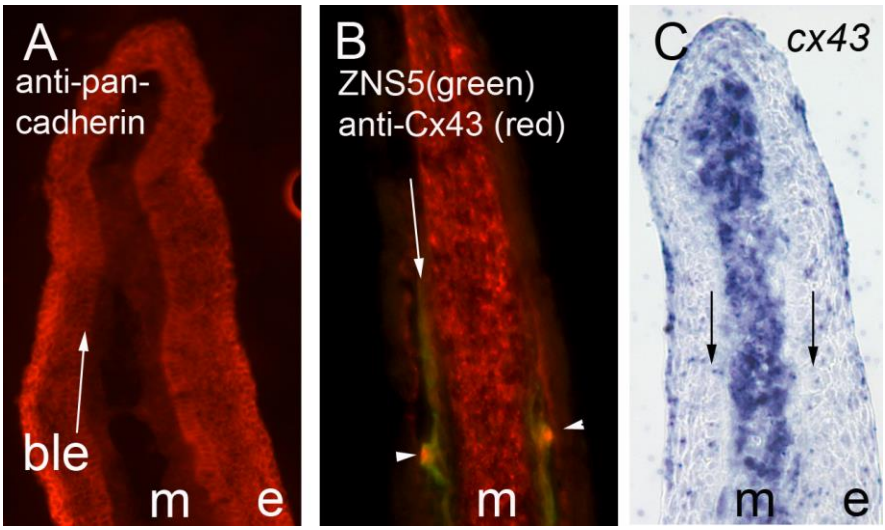

Figure 1.5: Longitudinal cryosections reveal fin compartments. (A) Cells of the epithelum are labeled with a pan cadherin antibody. Arrow points to basal layer of the epithelium (ble). (B) ZNS5 (green) labels skeletal precursor cells in the lateral compartment. Anti-Cx43 antibody (red) against Cx43 protein labels the mesenchyme. Arrowheads point to the doubly labeled joint. (C) The *cx43* mRNA is in the medial mesenchyme, concentrated more in the blastema. Arrows identify bone matrix; m: mesenchyme; e: epithelium.

1.7 References

Akimenko, M. A., et al., 2003. Old questions, new tools, and some answers to the mystery of fin regeneration. *Dev Dyn*. 226**,** 190-201.

Avaron F., Smith A., and Akimenko M. Chapter 9: Sonic hedgehog signaling in the developing and regenerating fins of zebrafish. *Landes Bioscience*. 2000; Shh and Gli Signaling and Development. ISBN: 978-0-387-39956-0.

Azevedo, A.S., et al., 2012. The regeneration capacity of the zebrafish caudal fin is not affected by repeated amputaitons. *PlosOne.* 6, (7): e820 21829525

Becerra, J., et al., 1983. Structure of the tail fin in teleosts. *Cell Tissue Res*. 230**,** 127-37.

Becerra, J., et al., 1996. Regeneration of fin rays in teleosts: A histochemical, radioautographic, and ultrastructural study. *Arch. Histol Cytol*. 59: 15–35.

Bivi, N., et al., 2012. Cell autonomous requirement of connexin 43 for osteocyte survival: consequences for endocortical resorption and periosteal bone formation. *J Bone Miner Res*. 27:374–389

Brown, A. M., et al., 2009. Osteoblast maturation occurs in overlapping proximal-distal compartments during fin regeneration in zebrafish. *Dev Dyn*. 238**,** 2922-8.

Chung, D. J., et al., 2006. Low peak bone mass and attenuated anabolic response to parathyroid hormone in mice with an osteoblast-specific deletion of connexin43. *J Cell Sci*. 119:4187–4198.

Dinsmore, E. C. Chapter 4: Abraham Trembley and the origins of research on regeneration in animals. *Cambridge University Press*. 1991. A history of regeneration research. ISBN: 0-521-04796-X.

Dobrowolski R.,et al., 2008. The conditional connexin43G138R mouse mutant represents a new model of hereditary oculodentodigital dysplasia in humans. *Hum Mol Genet*. 17:539–554.

Flenniken, A. M., et al., 2005. A Gja1 missense mutation in a mouse model of oculodentodigital dysplasia. *Development*. 132**,** 4375-86.

Gauron, C., et al., 2013. Sustained production of ROS triggers compensatory proliferation and is required for regeneration to proceed. *Sci Rep*. 3**,** 2084.

Hoptak-Solga, A. D., et al., 2007. Zebrafish short fin mutations in *connexin43* lead to aberrant gap junctional intercellular communication. *FEBS Lett*. 581**,** 3297-302.

Hoptak-Solga, A. D., et al., 2008. Connexin43 (GJA1) is required in the population of dividing cells during fin regeneration. *Dev Biol*. 317**,** 541-8.

Iovine, M. K., 2007. Conserved mechanisms regulate outgrowth in zebrafish fins. *Nat Chem Biol*. 3**,** 613-8.

Iovine, M. K., et al., 2005. Mutations in *connexin43* (GJA1) perturb bone growth in zebrafish fins. *Dev Biol*. 278**,** 208-19.

Iovine, M. K., Johnson, S. L., 2000. Genetic analysis of isometric growth control mechanisms in the zebrafish caudal Fin. *Genetics*. 155**,** 1321-9.

Ishida, T., et al., Phosphorylation of Junb family proteins by the Jun N-terminal kinase supports tissue regeneration in zebrafish. *Dev Biol*. 340**,** 468-79.

Johnson, S.L. and Bennett P. 1999. Growth control in ontogenetic and regenerating zebrafish fin. *Methods Cell Biol*. 59, 301-11.

Kawakami, A., 2010. Stem cell system in tissue regeneration in fish. *Dev Growth Differ*. 52**,** 77-87.

Knopf, F., et al., 2011. Bone regenerates via dedifferentiation of osteoblasts in the zebrafish fin. *Dev Cell*. 20**,** 713-24.

Kolodkin, A. L., et al., 1992. Fasciclin IV: sequence, expression, and function during growth cone guidance in the grasshopper embryo. *Neuron*. 9**,** 831-45.

Lecanda F., et al., 2000. Connexin43 deficiency causes delayed ossification, craniofacial abnormalities, and osteoblast dysfunction. *J Cell Biol*. 151:931–944.

Lee, Y., et al., 2005. Fgf signaling instructs position-dependent growth rate during zebrafish fin regeneration. *Development*. 132**,** 5173-83.

Makarenkova, H., et al., 1999. Gap junction signaling mediated through connexin-43 is required for chick limb development. *Dev Biol*. 207:380–392.

McGonnell, I.M., et al., 2001. Connexin43 gap junction protein plays an essential role in morphogenesis of the embryonic chick face. *Dev Dyn*. 222:420–438.

Nechiporuk, A., Keating, M. T., 2002. A proliferation gradient between proximal and *msxb*-expressing distal blastema directs zebrafish fin regeneration. *Development*. 129**,** 2607-17.

Paznekas, W. A., et al., 2003. Connexin 43 (GJA1) mutations cause the pleiotropic phenotype of oculodentodigital dysplasia. *Am J Hum Genet*. 72**,** 408-18.

Pfenniger, A., et al., 2010. Mutations in connexin genes and disease. *Eur J Clin Invest*. 41**,** 103-16.

Poss, K. D., et al., 2003. Tales of regeneration in zebrafish. *Dev Dyn*. 226**,** 202-10.

Poss, K. D., et al., 2002. Mps1 defines a proximal blastemal proliferative compartment essential for zebrafish fin regeneration. *Development*. 129**,** 5141-9.

Quint, E., et al., 2002. Bone patterning is altered in the regenerating zebrafish caudal fin after ectopic expression of *sonic hedgehog* and *bmp2b* or exposure to cyclopamine. *Proc Natl Acad Sci U S A*. 99**,** 8713-8.

Reaume A.G.; et al., 1995. Cardiac malformation in neonatal mice lacking connexin43. *Science.* 267:1831–1834.

Roth, L., et al., 2009. The many faces of semaphorins: from development to pathology. *Cell Mol Life Sci*. 66**,** 649-66.

Sims, K., Jr., et al., 2009. Connexin43 regulates joint location in zebrafish fins. *Dev Biol*. 327**,** 410-8.

Singh, S. P., et al., 2012. Regeneration of amputated zebrafish fin rays from de novo osteoblasts. *Dev Cell*. 22**,** 879-86.

Sousa, S., et al., 2011. Differentiated skeletal cells contribute to blastema formation during zebrafish fin regeneration. *Development*. 138**,** 3897-905.

Stains, J. P., et al., 2003. Gap junctional communication modulates gene transcription by altering the recruitment of Sp1 and Sp3 to connexin-response elements in osteoblast promoters. *J Biol Chem*. 278**,** 24377-87.

Stewart, S., et al., 2009. A histone demethylase is necessary for regeneration in zebrafish. *Proc Natl Acad Sci U S A*. 106**,** 19889-94.

Stoick-Cooper, C. L., et al., 2007. Advances in signaling in vertebrate regeneration as a prelude to regenerative medicine. *Genes Dev*. 21**,** 1292-315.

Thummel, R., et al., 2006. Inhibition of zebrafish fin regeneration using in vivo electroporation of morpholinos against *fgfr1* and *msxb*. *Dev Dyn*. 235**,** 336-46.

Ton, Q. V., Iovine, M. K., 2013. Determining how defects in *connexin43* cause skeletal disease. *Genesis*. 51**,** 75-82.

Ton, Q. V., Kathryn Iovine, M., 2012. Semaphorin3d mediates Cx43-dependent phenotypes during fin regeneration. *Dev Biol*. 366**,** 195-203.

Tu, S., Johnson, S. L., 2011. Fate restriction in the growing and regenerating zebrafish fin. *Dev Cell*. 20**,** 725-32.

van Eeden, F. J., et al., 1996. Genetic analysis of fin formation in the zebrafish, Danio rerio. *Development*. 123:255–262.

Watkins M., et al., 2011. Osteoblast connexin43 modulates skeletal architecture by regulating both arms of bone remodeling. *Mol Biol Cell* 22:1240–1251.

Wolman, M. A., et al., 2004. Repulsion and attraction of axons by *semaphorin3D* are mediated by different neuropilins in vivo. *J Neurosci*. 24**,** 8428-35.

Zhang, Y., et al., 2012. Enhanced osteoclastic resorption and responsiveness to mechanical load in gap junction deficient bone. *PLoS One*. 6:e23516.

CHAPTER 2

Semaphorin3d Mediates Cx43-Dependent Phenotypes During Fin Regeneration

2.1 Abstract

Gap junctions are proteinaceous channels that reside at the plasma membrane and permit the exchange of ions, metabolites, and second messengers between neighboring cells. Connexin proteins are the subunits of gap junction channels. Mutations in zebrafish *cx43* cause the *short fin* (*sof*^{b123}) phenotype which is characterized by short fins due to defects in length of the bony fin rays. Previous findings from our lab demonstrate that Cx43 is required for both cell proliferation and joint formation during fin regeneration. Here we demonstrate that *semaphorin3d* (*sema3d*) functions downstream of Cx43. Semas are secreted signaling molecules that have been implicated in diverse cellular functions such as axon guidance, cell migration, cell proliferation, and gene expression. We suggest that Sema3d mediates the Cx43-dependent functions on cell proliferation and joint formation. Using both in situ hybridization and quantitative RT-PCR, we validated that *sema3d* expression depends on Cx43 activity. Next, we found that knockdown of Sema3d recapitulates all of the *sof*^{b123} and *cx43*-knockdown phenotypes, providing functional evidence that Sema3d acts downstream of Cx43. To identify the potential Sema3d receptor(s), we evaluated gene expression of *neuropilin*s and *plexins*. Of these, *nrp2a*, *plxna1*, and *plxna3* are expressed in the regenerating fin. Morpholino-mediated knockdown of *plxna1* did not cause *cx43*-specific defects, suggesting that PlexinA1 does not function in this pathway. In contrast, morpholino-mediated knockdown of *nrp2a* caused fin overgrowth and increased cell proliferation, but did not influence joint formation. Moreover, morpholino-mediated knockdown of *plxna3* caused short segments,

influencing joint formation, but did not alter cell proliferation. Together, our findings reveal that Sema3d functions in a common molecular pathway with Cx43. Furthermore, functional evaluation of putative Sema3d receptors suggests that Cx43-dependent cell proliferation and joint formation utilize independent membrane-bound receptors to mediate downstream cellular phenotypes.

2.2 Introduction

Connexins are the subunits of gap junction channels that direct cell-cell communication of ions and metabolites (≤1200 Da). Each connexin is a four-pass transmembrane spanning domain protein. Six connexins oligomerize to form a hemichannel, or connexon. Two connexons dock at the plasma membrane of adjacent cells to form a complete gap junction channel. Gap junction intercellular communication (GJIC) contributes to numerous developmental processes, including skeletogenesis. For example, mutations in human *CX43* result in oculodentodigital dysplasia (ODDD, Paznekas et al., 2003). ODDD is an autosomal dominant disease causing craniofacial bone deformities and limb abnormalities (Paznekas et al., 2003; Flenniken et al., 2005). Skeletal defects in the $CX43^{-/-}$ knockout mouse include delayed ossification of the axial and craniofacial skeletons (Lecanda et al., 2000). However, the underlying mechanisms by which Cx43-based GJIC leads to skeletal disease phenotypes are largely unknown.

Importantly, the function of Cx43 in skeletal morphogenesis is conserved. Indeed, our lab has found that mutations in zebrafish *cx43* cause the *short fin* (sof^{b123}) phenotype (Iovine et al., 2005). The sof^{b123} mutant is characterized by defects in the length of the bony fin ray segments, leading to short fins. The sof^{b123} allele exhibits reduced *cx43* mRNA levels without a lesion in the coding sequence (Iovine et al., 2005). However, three additional alleles generated by non-complementation express missense mutations that cause reduced GJIC (Hoptak-Solga et al., 2007). During fin regeneration, the *cx43* mRNA is up-regulated in the population of dividing cells.

Indeed, all four *sof* alleles exhibit reduced levels of cell proliferation in addition to short segments (Hoptak-Solga et al., 2008). Furthermore, morpholino-mediated *cx43* knockdown completely recapitulates the reduced fin length, reduced segment length, and reduced cell proliferation phenotypes observed in the *sof* alleles (Hoptak- Solga et al., 2008). Together, these data reveal that reduced mRNA expression (*sof* ^{b123}), reduced protein expression (*sof* ^{b123}and morpholino-mediated knockdown), or reduced Cx43-based GJIC (three missense alleles) cause the same set of phenotypes. Thus, we refer to any loss of Cx43 function as a loss of Cx43 activity.

Given the observation that any loss of Cx43 activity leads to both reduced cell proliferation and short segments, it may be natural to speculate that reduced cell proliferation causes short segments. However, reduced signaling via the Shh or Fgfr1 signaling pathways also causes reduced cell proliferation and reduced fin length, but does not influence segment length (Quint et al., 2002; Lee et al., 2005). Thus, reducing the level of cell proliferation is not sufficient to impact segment length. We suggest instead that Cx43 plays an additional role in the regulation of segment length, perhaps by regulating joint formation. Our analyses of the *another long fin* (*alf* ^{dty86}) mutant supports this hypothesis. In contrast to *sof*, the *alf* ^{dty86} mutant exhibits fin overgrowth and stochastic joint failure/overlong segments (van Eeden et al., 1996), phenotypes opposite to *sof*. Interestingly, our analyses revealed that *alf* ^{dty86} mutants over-express *cx43* mRNA (Sims et al., 2009). Furthermore, *cx43*- knockdown in *alf* ^{dty86} fins rescues overgrowth and segment length, suggesting that *cx43* over-expression is responsible for the *alf* ^{dty86} phenotypes (Sims et al., 2009). Based on these loss-of-function and gain-

of-function phenotypes, we suggest that Cx43 activity promotes cell proliferation and suppresses joint formation, thereby coordinating bone growth and skeletal patterning.

A long-standing question with regard to connexin mutations is, *how* do gap junctions influence tangible cellular outcomes such as cell proliferation and cell differentiation? One hypothesis is that Cx43-based GJIC influences gene expression (Stains et al., 2003). To identify global changes in gene expression occurring downstream of *cx43*, we utilized a novel microarray strategy. We focused on the subset of genes both down-regulated in *sof* ^{b123} and up-regulated in *alf* ^{dty86} to enable the identification of *cx43*-dependent genes. Here we provide molecular and functional validation of one gene identified by this microarray, *semaphorin3d* (*sema3d*). Semas comprise a large family of evolutionarily conserved signaling molecules initially found to provide axonal guidance cues during patterning of the central nervous system (Kolodkin et al., 1992). More recent studies have revealed that semaphorins are expressed in most cell types and, in addition to patterning the nervous system, also contribute to vasculature, heart, lung, kidney, bone and tooth development (reviewed in Roth et al., 2009). Class 3 Semas, such as Sema3d, are secreted ligands that interact with several possible cell surface receptors in order to mediate downstream cellular outcomes including cell adhesion, cell migration, cell proliferation, cell viability, and gene expression (reviewed in Yazdani and Terman, 2006). Thus, the finding that a Semaphorin acts functionally downstream of Cx43 provides tangible insights into how skeletal morphogenesis may be influenced by Cx43 activity.

2.3 Materials and Methods

Fish maintenance

Zebrafish were raised at constant temperature of 25 ^{o}C with 14 light: 10 dark photoperiod (Westerfield, 1993). Wild-type (C32), *sof* ^{b123} (Iovine and Johnson, 2000) and *alf* ^{dyt86} (van Eeden et al., 1996) were used in this study.

RNA isolation, fluorescent cRNA synthesis and microarray hybridization

Total RNA of wild-type, *sof* ^{b123} and *alf* ^{dty86} 5 dpa regenerating fins were extracted using Trizol (Invitrogen, San Diego). RNA quantity and quality were determined by nanodrop and Bioanalyzer 2100 (Agilent) analyses. Only samples in yield higher than 50 ng/uL RNA, having sharp 60S and 40S rRNA peaks shown in the Bioanalyzer electropheretogram, and 260/280 ratios > 1.7 were used. Fluorescent cRNAs were generated using the Agilent Low RNA Input Linear Amplification Kit and Qiagen RNeasy mini columns to purify the fluorescent target. Experimental Cy5 labeled samples (*alf* ^{dty86}, *sof* ^{b123}) were competitively hybridized against equal amounts of Cy3 labeled wild-type cRNAs on an Agilent 4x44K zebrafish 60-mer oligo microarray (G25190F-015064). After careful washing the microarray was scanned in an Agilent microarray scanner and red (Cy5) and green (Cy3) signal intensities were evaluated and processed with Agilent Feature Extraction software (v 7.5). The relative expression value of a gene for two different samples was represented by base 2 log ratios of the two signal intensities.

Further data normalization, transformation and filtering for differential gene expression were performed using Agilent Genespring GX (v7.5).

In situ hybridization

Probes were prepared from linear DNA generated from PCR products where the reverse primer contained the binding site for the T7 RNA polymerase (see Table 2.1 for sequences). Five days post amputation (dpa) regenerating fins from wild-type, *sof*^{b123}, or *alf*^{dty86} were fixed overnight with 4% paraformaldehyde in PBS and dehydrated in 100% methanol at -20 ^{o}C. Gradual aqueous washes were completed in methanol/PBST. Fins were then treated with 5 μg/ml proteinase K for 45 minutes and re-fixed in 4% paraformaldehyde in PBS for 20 minutes. Extensive washes in PBST were followed by prehybridization process in HYB+ solution (HYB+ solution is consisted of 50% formamide, 5 X SSC, 10 mM citric acid, 0.1% Tween20, heparin and tRNA) at 65 ^{o}C for 30 minutes – 1 hour. Hybridization in the presence of digoxigenin-labeled antisense probes was completed overnight at 65 ^{o}C. The next day, the fins were washed gradually in HYB- to 2X SSC to 0.2X SSC and finally to PBST. Anti-digoxigenin Fab fragments (pre-absorbed against zebrafish tissue) were used at 1:5,000 overnight. On day 3, extensive washes in PBST were performed before three short washes in staining buffer (100 mM Tris, 9.5, 50 mM $MgCl_2$, 100 mM NaCl, 0.1 % Tween20, pH 9.0). Fins were next transferred to staining solution (staining buffer plus NBT and BCIP) and development proceeded until a purple color was observed. For final result, fins were then washed with PBST, pre-fixed in 4% paraformaldehyde in PBS and mounted onto microscope slides. Labeled fins were examined on a Nikon Eclipse 80i microscope. Images were collected using a digital Nikon camera.

Following whole mount in situ hybridization, fins were embedded in 1.5%

agarose/5% sucrose, and equilibrated overnight in 30% sucrose. Fins were mounted in OCT and cryosectioned (18–20 µm sections) using a Reichert-Jung 2800 Frigocut cryostat. Sections were collected on Superfrost Plus slides (Fisher) and mounted in 100% glycerol.

Morpholino Knockdown and Electroporation

Injection and Electroporation experiments were performed as described (Thummel et al., 2006; Hoptak-Solga et al., 2008; Sims et al., 2009). Targeting morpholinos were targeted against the start codon and modified with fluorescein (Gene Tools, LLC) to provide a charge and for detection. Sequences for the targeting and control morpholinos can be found in Table 2.1.

Adult fish were first anesthetized using Tricane-S. Fin amputation was performed under a dissecting microscope. At 3 dpa, morpholinos were injected using a Narishige IM 300 Microinjector. Approximately 50 nl of morpholino (i.e. targeting or control 5MM morpholinos) was injected per ray (5- 6 fin rays per fin, the other rays were uninjected control). Immediately following injection, both dorsal and ventral halves were electroporated using a CUY21 Square Wave Electroporator (Protech International, Inc.). The following parameters were used: ten 50-ms pulses of 15 V with a 1 s pause between pulses. At 24 hpe (hours post electroporation), success was evaluated by monitoring fluorescein uptake under fluorescence microscope. Fins were harvested either at 1 dpe for H3P detection and for qRT-PCR or at 4 dpe for ZNS5 detection. Three to five fins were injected per morpholino (i.e. targeting or mismatch); the un-injected side served as an independent control. Each morpholino was tested in

at least three independent experiments to ensure reproducibility. The graphs in Figure 2.2 are based combined data from two comparable experiments (n = 7). Statistical significance was determined using the student's t-test ($p<0.05$).

Immunofluorescence

Fins were harvested after morpholino knockdown experiments (for ZNS5 detection staining, fins were harvested 4 dpe; for H3P detection staining, fins were harvested 1 dpe). Fins were then fixed in 4% paraformaldehyde in PBS for 2 hours at RT and then dehydrated in methanol. During processing, fins were washed gradually in methanol/PBS followed by 3 washes in block solution (50 ml PBS, 1 g BSA, 250 µl triton). Either the mouse ZNS5 (Zebrafish International Resource Center: http://zebrafish.org/zirc/home/guide.php, 1:200) or the rabbit antibody against histone-3-phosphate (anti-H3P, Millipore, 1:100) were incubated with fins overnight at 4 ^{o}C. Next day, antibodies were removed and fins were washed in block solution 3x10 minutes. Secondary antibodies (i.e. anti-mouse Alexa 488 for ZNS5 detection or anti-rabbit Alexa 546 for H3P detection) were diluted in 1:200 blocking solution and incubated overnight at 4 ^{o}C. Following 3x10 minutes treatment in blocking solution, fins were washed in PBS and then mounted onto slides in glycerol. Labeled fins were examined on a Nikon Eclipse 80i microscope. Images were collected using a digital Nikon camera.

Measurements

Fins were imaged on a Nikon SMZ1500 dissecting microscope at 4X (regenerate length) or 10X (segment length or the number of dividing cells).

Photographs were taken using a Nikon DXM1200 digital camera. For regenerate length, segment length, and the number of dividing cells, all measurements were taken from only the longest fin rays (i.e. the third ray from either the dorsal or ventral end) since that was previously established as a standard (Iovine and Johnson, 2000). Student's t- tests were performed in Excel to determine if experimental conditions were significantly different from control conditions.

Regenerate and segment length was measured using ImagePro software. Fin ray length was measured from the amputation plane (clearly visible in bright field) to the end of the fin. Segment length is measured as the distance between two joints where joints are identified (i.e. and clearly distinguished from breaks) following ZNS5 staining (Sims et al., 2009).

The mitotic cells were first detected by H3P staining as described above (i.e. Histone-3 is phosphorylated on Ser10 only during mitosis, Wei et al., 1999). H3P positive cells were counted from within the distal-most 250 μm of each ray (Hoptak-Solga et al., 2008).

qRT-PCR Analysis

qRT-PCR analysis was performed as described (Sims et al., 2009). In brief, Trizol reagent was used to isolate mRNA from 5 dpa wild-type, *sof* ^{b123}, or *alf* ^{dty86} regenerating fins and 1 dpe (i.e. *cx43*- knockdown fins) (5 fins per pool). First strand cDNA was synthesized using oligodT (12-15) and reverse transcriptase. Dilution of template cDNA (1:10) was prepared. Oligos flanking introns were designed for *sema3d* (F-5' TGGATGAGGAGAGAAGCCGAT 3'; R-5' GCAGGCCAGCTCAACTTTTT

3') using Primer Express software (primers for *cx43* and *keratin4* can be found in Sims et al., 2009). The *sema3d*, *cx43*, and *keratin4* amplicons were amplified independently using the Power SYBR green PCR master mix (Applied Biosystems). Samples were run in triplicate on the ABI7300 Real Time PCR system and the average cycle number (C_T) was determined for each amplicon. Delta C_T (ΔC_T) values represent normalized *sema3d* levels with respect to *keratin4*, the internal control. The relative level of gene expression was determined using the delta delta C_T ($\Delta\Delta C_T$) method (i.e. $2^{-\Delta\Delta CT}$). A minimum of three trials were run to ensure the reproducibility of the results.

2.4 Results

sema3d functions downstream of cx43

We completed a novel microarray strategy designed to identify genes acting downstream of *cx43*. We took advantage of our findings that *cx43* expression is reduced in *sof* ^{b123} and increased in *alf* ^{dty86} in order to identify a group of genes that are both down-regulated when *cx43* is down-regulated (i.e. in *sof* ^{b123}) and up-regulated when *cx43* is up-regulated (i.e. in *alf* ^{dty86}). Importantly, the *cx43* gene is found among the top 50 genes identified using this strategy, strongly suggesting that this approach identified relevant genes of interest. Another gene found in the top half of the microarray was *sema3d*. Given the importance of semaphorins in a diversity of signaling pathways, we were intrigued at the possibility that Sema3d signaling mediates Cx43 activities.

In order to validate *sema3d* as a downstream target of *cx43*, we first examined *sema3d* expression in wild-type, *sof* ^{b123} and *alf* ^{dty86} regenerating fins by whole mount in situ hybridization. As anticipated, *sema3d* mRNA expression appeared down-regulated in *sof* ^{b123} and up-regulated in *alf* ^{dty86} (Figure 2.1). Next, we determined the tissue-specific expression of *sema3d* as revealed by cryosectioning. The outer cell layers of the fin are epidermis; the basal layer of the epidermis is identified as a row of cuboidal-shaped cells closest to the mesenchymal compartment. Within the mesenchyme, the skeletal precursor cells (i.e. pre-osteoblasts and pre-joint-forming cells) are located laterally. The regeneration blastema, the specialized population of dividing cells contributing to new fin outgrowth, is medially adjacent to the skeletal

precursors. This population of cells up-regulates *cx43* expression during fin regeneration (Hoptak-Solga et al., 2008). In contrast, cryosectioning of stained *sema3d*-positive fins revealed that *sema3d* is expressed in both the lateral skeletal precursor cells and in the lateral basal layer of the epidermis (Figure 2.1). Since *sema3d* expression is not up-regulated in the *cx43*-positive cells, *sema3d* appars not to be a direct target of Cx43 activity.

To confirm the observed qualitative differences in *sema3d* expression we performed quantitative RT-PCR (qRT-PCR). We find that *sema3d* is reduced in *sof* ^{b123} and increased in *alf* ^{dty86} (Table 2.2). Moreover, we find that *sema3d* expression is reduced in wild-type fins treated for *cx43*-knockdown, providing independent evidence that *sema3d* expression is influenced by Cx43 activity. Together, these data support the hypothesis that *sema3d* expression is regulated by the level of Cx43.

Sema3d mediates Cx43-dependent cell proliferation and joint formation

To determine if *sema3d* mediates Cx43-dependent phenotypes, we completed morpholino- mediated gene knockdown of *sema3d* (as described for *cx43* knockdown in Hoptak-Solga et al., 2008 and in Sims et al., 2009). Briefly, fins were injected with either a gene-specific targeting morpholino (MO) or with an altered morpholino that includes five mismatches (MM) to the target sequence. Following injection into the distal region of the regenerate, fins were electroporated to permit cellular uptake. Morpholinos were modified with fluorescein, which both provides a requisite charge for electroporation and provides a method to confirm cellular uptake. Interestingly, we find that *sema3d*-knockdown exhibits all of the same loss-

of-function phenotypes as *sof*^{b123} mutants (Iovine et al., 2005;Hoptak-Solga et al., 2008) and as *cx43*-knockdown (Hoptak-Solga et al., 2008; Sims et al., 2009). Thus, *sema3d* knockdown fins exhibit reduced fin length, reduced segment length, and reduced cell proliferation (Figure 2.2 A-C and Figure 2.3 for representative images). The level of cell proliferation was evaluated by counting the number of cells in mitosis, detected using an antibody against histone-3- phosphate (i.e. H3P). These data demonstrate that *sema3d* mediates *cx43*-dependent fin phenotypes influencing growth and joint formation. To provide additional evidence that *sema3d* functions in a common pathway with *cx43*, we next attempted to rescue the joint formation phenotype of *alf*^{dty86}.

Indeed, *sema3d* knockdown rescued the joint failure phenotype of *alf*^{dty86}, causing reduced segment length (Figure 2.2D). Until now, only reduced *cx43* function has been associated with segment length phenotypes and with rescue of joint formation in *alf*^{dty86}. Therefore, the finding that *sema3d* knockdown caused short segments in wild-type and rescued segment length in *alf*^{dty86}is striking. Together these data indicate that *cx43* and *sema3d* function in a common pathway to regulate cell proliferation and joint formation. Thus, Sema3d signaling mediates Cx43-specific effects.

Identification of putative Sema3d receptors

Neuropilins (Nrps) and Plexins (Plxns) are likely receptors for Semaphorin signaling (reviewed in Zhou et al., 2008). Indeed, Nrps and Plxns may hetero-oligomerize to transduce Sema signals. Nrps are believed to bind Semas directly (although Plxns also contain a sema domain), but have a very short intracellular domain

that may not be sufficient to transduce intracellular signals. Plxns, on the other hand, have an extensive intracellular domain (reviewed in Zhou et al., 2009). Since both Nrps and Plxns are the best known receptors for Semas, we initiated a candidate gene search of these gene families. The zebrafish genome contains 4 *neuropilin* (*nrp*) genes (*nrp1a*, *nrp1b*, *nrp2a*, and *nrp2b*, Yu et al., 2004). In addition, Plexins in the A and D families are candidate receptors for secreted Semas (Zhou et al., 2008). The zebrafish genome contains *plexina1* (*plxna1*), *plxna3*, *plxna4*, and *plxnd1*. Of these 8 candidate genes, only *nrp2a*, *plxna1*, and *plxna3* appear to be expressed in regenerating fins by in situ hybridization (Figure 2.4). The expression of *nrp2a* appears mainly in the blastema, perhaps more heavily localized distally. The distal-most blastema has been proposed to regulate fin outgrowth during regeneration (Nechiporuk and Keating, 2002). There is also apparent staining in the skeletal precursor cells, and sporadic but strong staining in individual cells of the outer layers of the epithelium. The identity of these cells is not known. The *plxna1* gene is expressed primarily in the distal blastema and also in the distal basal layer of the epidermis. In contrast, *plxna3* appears to be expressed primarily in the skeletal precursor cells and throughout the medial compartment of the regenerate.

PlxnA3 and Nrp2a mediate independent Sema3d functions

Next we completed functional analyses to determine which, if any, of these receptors contribute to the Cx43-Sema3d pathway. Receptors that mediate Sema3d function are expected to exhibit similar knockdown phenotypes as *cx43* and *sema3d*. However, knockdown of *plxna1* did not appear to influence either cell proliferation or joint formation (Figures 2.2 and 2.3), suggesting that PlxnA1 does not participate in

Cx43-Sema3d-dependent skeletal morphogenesis. In contrast, knockdown of *plxna3* caused short segments (Figure 2.2C and Figure 2.3) but had no effect on cell proliferation (Figure 2.2B). There is some influence of *plxna3* knockdown on fin length, as the length of the regenerate was statistically shorter than the controls (Figure 2.2A). Since there was no effect on cell proliferation, we conclude that the small *plxna3*-dependent effect on fin length is due to its influence on segment length, and not on fin growth. To provide further support for the functional relationship between *plxna3* and *cx43*-dependent joint formation, we evaluated the effect of *plxna3*-knockdown in *alf* ^{dty86} regenerating fins. As anticipated, *plxna3*-knockdown rescued the joint formation phenotype, recapitulating the *cx43*- and *sema3d*-knockdown effects (Figure 2.2D). These data suggest that PlxnA3 contributes to Sema3d- mediated joint formation. Therefore, we have now identified a third gene (i.e. *plxna3*), predicted to function downstream of Cx43-Sema3d, whose function is required for appropriate joint formation.

Knockdown of *nrp2a* caused increased fin growth and increased cell proliferation (Figure 2.2A,B and Figure 2.3), suggesting that signaling via Nrp2a negatively influences cell division. There was no effect on segment length following *nrp2a* gene knockdown (Figure 2.2C), indicating that Nrp2a signaling does not mediate Sema3d effects on joint formation. Since knockdown of *cx43* and *sema3d* both cause reduced growth and reduced cell proliferation, it was anticipated that Nrpa2a knockdown would similarly cause reduced growth and cell proliferation. Since this was not the case, we suggest instead that Sema3d binding to the Nrp2a receptor

inactivates its activity, thereby positively regulating cell division by inhibiting a negative signal. We attempted to provide evidence for this hypothesis by evaluating Nrpa2a knockdown in *sof*^{b123} fins, which express less *sema3d* (Figure 2.1 and Table 2.2). For example, if Sema3d is required to block the effects of Nrp2a signaling, then the increase in cell proliferation associated with Nrp2a knockdown should be attenuated when Sema3d is reduced, as in *sof*^{b123}. This is what we find. Nrp2a knockdown in wild-type regenerating fins causes a 30 % increase in dividing cells, while Nrp2a knockdown in *sof*^{b123}regenerating fins has no effect on the number of dividing cells (Figure 2.5). Further studies will be required to demonstrate unequivocally that Sema3d acts as a ligand for Nrp2a. However, our current findings provide support for the conclusion that Sema3d can mediate negative regulation of Nrp2a and thereby promote cell proliferation. Note that the observed Nrp2a effects may be mediated in conduction with an as yet unidentified Plxn co-receptor since Nrps appear not to encode intracellular signaling domains.

Together, our analyses of the *plxna1*, *plxna3*, and *nrp2a* genes suggest that Nrp2a and PlxnA3 mediate Sema3d-dependent events, while PlxnA1 does not appear to function in Sema3d-mediated events. Moreover, we suggest that Nrp2a and PlxnA3 mediate distinct Cx43- and Sema3d-dependent phenotypes, where Nrp2a mediates the Cx43-dependent effects on cell proliferation and PlxnA3 mediates the Cx43 dependent effects on joint formation.

2.5 Discussion

Much of what is known about *sema3d* has been determined during development of the central nervous system in zebrafish. In the embryonic nervous system *sema3d* has been found to exert multiple diverse functions. For example, *sema3d* may act as an axonal repellent or as an axonal attractant (Wolman et al., 2004). Alternatively, *sema3d* function can modify cell adhesion via influencing the expression of the adhesion protein L1 (Wolman et al., 2007). Further, *sema3d* has been found to influence the population of neural crest cells by promoting proliferation (Berndt and Halloran, 2006), and by regulating their migration (Yu and Moens, 2005). It has been suggested that the different functions of *sema3d* may depend on the receptors expressed on the responding cells. Indeed, depending on the cell-type, *sema3d* has been found to interact with *nrp1a* (Wolman et al., 2004), with *nrp1a*/*nrp2b* (Wolman et al., 2004), or via *nrp*-independent mechanisms (Wolman et al., 2007). Thus, Sema3d appears to interact with a variety of receptors in order to mediate a diversity of downstream cellular events. It is therefore not possible to predict a specific receptor complement/pathway for Sema3d function. However, it is also not difficult to envision how Sema3d signaling could be responsible for mediating multiple independent signaling events during fin regeneration.

The finding that Sema3d functions downstream of Cx43 is supported by multiple independent lines of evidence. First, the *sema3d* gene exhibits differential expression in *sof* ^{b123} and *alf* ^{dty86} regenerating fins by in situ hybridization and by qRT-PCR. Second, *cx43*-knockdown in wild-type fins is sufficient to reduce *sema3d* gene

expression. Third, we provide functional evidence that *sema3d* acts downstream of *cx43* since *sema3d*-knockdown recapitulates all of the *cx43*-dependent phenotypes, including rescue of joint formation in *alf*^{dty86}. Thus, *sema3d* is both molecularly and functionally downstream of Cx43. Moreover, we identify two putative Sema3d receptors, Nrp2a and PlxnA3. Remarkably, these receptors appear to independently mediate Cx43-Sema3d-dependent cell proliferation and joint formation. The described functional analyses for Sema3d and its putative receptors utilized translation-blocking morpholinos. Since antibodies are not currently available, we are unable to demonstrate that protein translation of the targets is inhibited following morpholino-mediated gene knockdown. However, the specificity of *sema3d*- and *plxna3*- knockdown to Cx43-dependent phenotypes is provided by our findings that *sema3d*- and *plxna3*-knockdown both cause short segments and also rescue joint failure in *alf*^{dty86} (i.e. prior to this report, these findings were specific for *cx43* mutations or knockdown). Similarly, the finding that *sof*^{b123} abrogates the effects of *nrp2a*-knockdown provides specificity for the role of Nrp2a in Cx43-Sema3d-dependent cell proliferation. We did not observe Cx43-dependent phenotypes following *plxna1*-knockdown. However, until we can demonstrate that the PlxnA1 protein has been successfully reduced, we cannot formally rule out the possibility that PlxnA1 also contributes to Sema3d signaling events.

Based on our current and published findings (summarized in Table 2.3), we suggest the following model for Cx43 activity during fin regeneration (Figure 2.6). Prior studies from our lab have shown that Cx43 both promotes cell proliferation and suppresses joint formation (Hoptak-Solga et al., 2008; Sims et al., 2009). Here we find

that Sema3d signaling contributes to these Cx43-dependent activities in a pathway that bifurcates after Sema3d (Figure 2.6A). Indeed, functional analyses of Cx43 and Sema3d provide evidence that cell proliferation and joint formation are coupled, while functional analyses of the putative Sema3d receptors demonstrate effects on either cell proliferation (i.e. Nrp2a) or joint formation (PlxnA3). Thus, Cx43 coordinates skeletal growth and patterning via Sema3d signaling, which in turn regulates cell proliferation and joint formation in distinct downstream signaling pathways.

It is possible to visualize the steps of this molecular pathway by considering the location of gene expression of the molecular players (Figure 2.6B). For example, Cx43 is expressed in the medially located dividing cells during fin regeneration (Iovine et al., 2005). These cells are directly adjacent to the skeletal precursor cells that will differentiate as either osteoblasts or joint forming cells (Brown et al., 2009; Borday et al., 2001). We suggest that Cx43 activity in the dividing cells influences gene expression of *sema3d* in the adjacent lateral compartments, which in turn mediates independent signaling pathways that regulate cell division and joint formation. It remains unknown how gap junctions contribute to tangible changes in gene expression. One possibility is that Cx43-dependent GJIC influences the concentration of a second messenger that directly regulates the activity of a relevant transcription factor in the *cx43*-positive cells. These changes in gene expression in the *cx43*-positive compartment lead to changes in gene expression in the adjacent *sema3d*-positive compartment. Once the expression of *sema3d* is up-regulated in the lateral skeletal precursor cells, Sema3d will be secreted where it may interact with its receptors.

Conveniently, Nrp2a and PlxnA3, which mediate independent events, are expressed in distinct populations of cells. For example, the Nrp2a receptor is expressed in the distal blastema where it may influence cell proliferation in the *cx43*-positive cells. We suggest that Sema3d binding to Nrp2a prevents the inhibition of cell proliferation, thereby promoting growth. Similarly, the expression of *plxna3* in the skeletal precursor cells suggests that secreted Sema3d binds to the PlxnA3 receptor and initiates an autocrine response to influence the expression of genes that will determine joint formation (i.e. promoting osteoblast differentiation, suppressing joint formation, or both). However, recall that *nrp2a* and *plxna3* are expressed in more than one cellular compartment during fin regeneration. Thus, it remains possible that Sema3d signaling events are more complicated than this model suggests.

The model we propose suggests that Sema3d initiates a typical signal transduction pathway that directly influences cell proliferation or joint formation in the cells expressing the putative receptors. This model is consistent with our examination of gene expression patterns and on functional analyses. Alternate models are also possible. For example, it has been suggested that Sema3A influences innervation and/or vasularization of endochondral bones in mammals, which in turn impacts bone growth (Gomez et al., 2005). The fin rays contain both nerve axons and blood vessels, although it is not known if Sema3d and/or its receptors are expressed in either of those cell populations. Future immunohistochemical analyses may provide new insights into the possibility that Cx43-Sema3d drives growth and/or patterning via the vasculature or nervous system. Moreover, others have found evidence that Sema3F may influence the

localization of Cx43 to the plasma membrane in rat liver epithelial cell lines, perhaps regulating Cx43-based GJIC (Kawasaki et al., 2007). Our findings do not support this type of role for Sema3d during fin regeneration since *cx43* and *sema3d* are not co-expressed in the same population of cells. However, it remains possible that additional Semas may contribute to the expression and/or localization of Cx43.

2.6 Conclusions

The identification of Sema3d acting downstream of Cx43 provides tangible insights into how cellular outcomes are coupled in order to coordinate bone growth with skeletal patterning. We find that the Cx43-Sema3d pathway diverges via distinct receptors to influence two cellular outcomes: cell proliferation and joint formation. Continued validation of additional genes identified by our microarray will fill the gaps of molecular events occurring both between Cx43 activity and Sema3d signaling as well as events occurring downstream of the putative Sema3d receptors that mediate changes in cell division and joint formation.

2.7 Figures

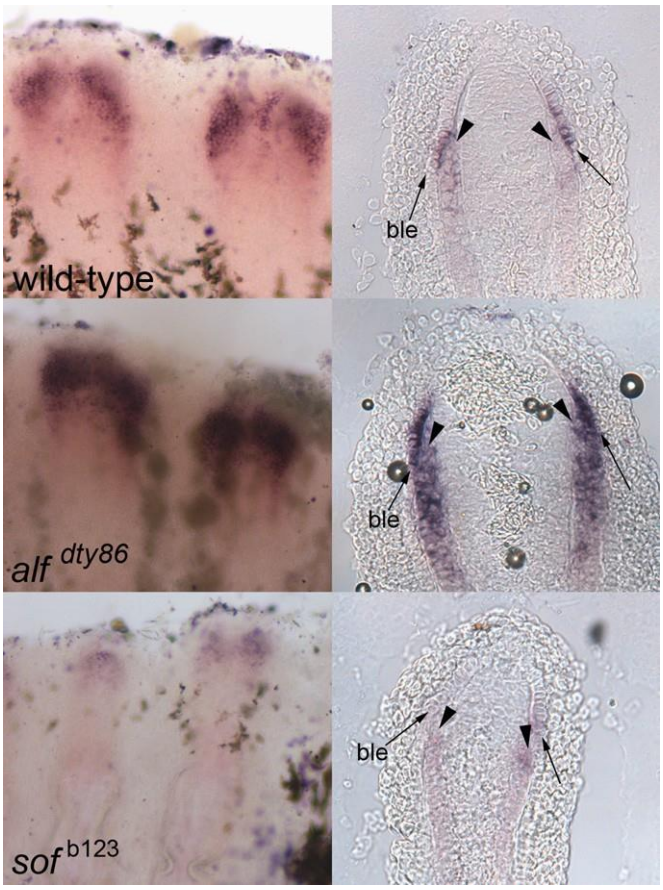

Figure 2.1 *sema3d* is differentially expressed in wild-type (top), *alf* ^{dty86} (middle) and *sof* ^{b123} (bottom). Left: whole mount in situ hybridization shows increased expression in *alf* ^{dty86} and decreased expression in *sof* ^{b123} compared to wild-type. Right: Cryosections reveal the tissue-specific localization of *sema3d*-expressing cells. Arrowheads point to skeletal precursor cells; arrows point to the basal layer of the epidermis (ble)

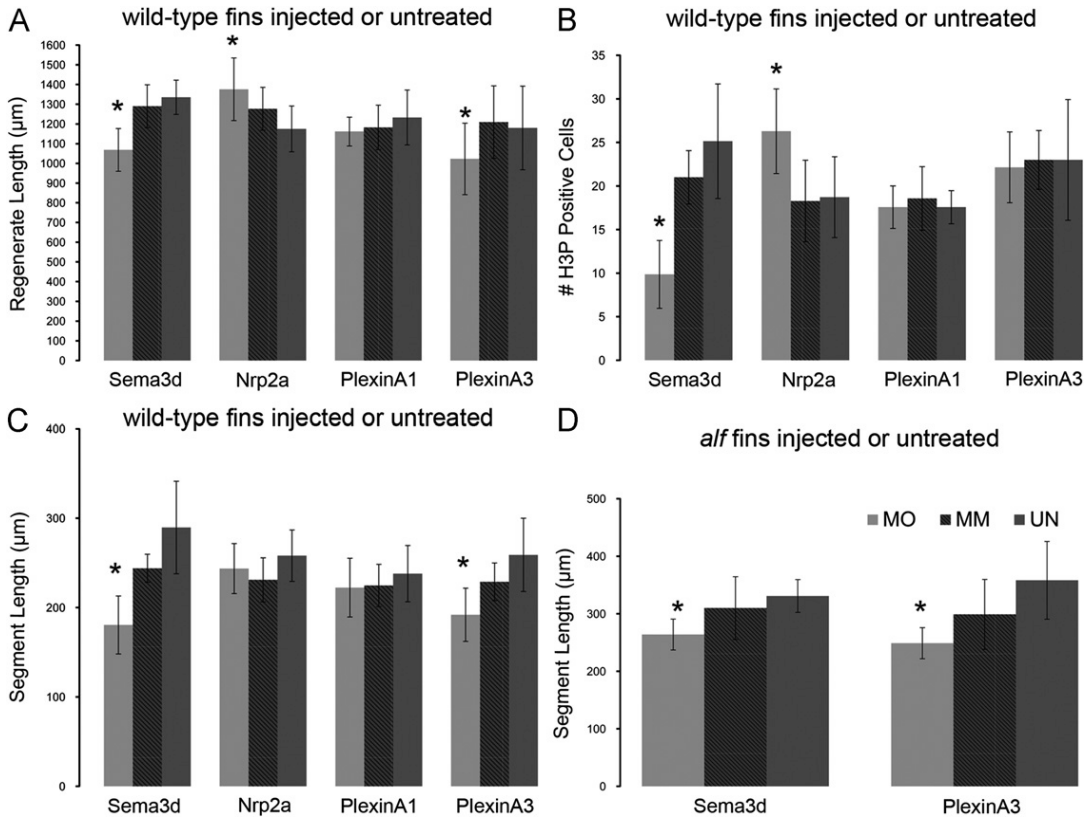

Figure 2.2 Morpholino-mediated gene knockdown of *sema3d* and its putative receptors. In all graphs, MO represents the particular gene-targeting morpholino; MM represents the particular 5 mis-match/control morpholino; UN represents uninjected/untreated fins. (A) Total regenerate length was measured. *sema3d*-knockdown and *plxna3*-knockdown cause reduced fin length (*); *nrp2a*-knockdown causes increased fin length (*), (B) the total number of H3P positive cells were counted. *sema3d*-knockdown causes reduced levels of cell proliferation (*); *nrp2a*-knockdown causes increased levels of cell proliferation (*), (C) segment length was measured in treated wild-type fins. *sema3d*-knockdown and *plxna3*-knockdown cause reduced segment length (*) and (D) segment length was measured in treated *alf* ^{dty86} fins. *sema3d*-knockdown and *plxna3*-knockdown cause reduced segment length and rescue joint formation in *alf* ^{dty86} (*). Statistically different data sets (*) were determined by the student's t-test where $p<0.05$. By the student's t-test, there is no statistical difference between MM and UN for any mismatch morpholino. Error bars represent the standard deviation.

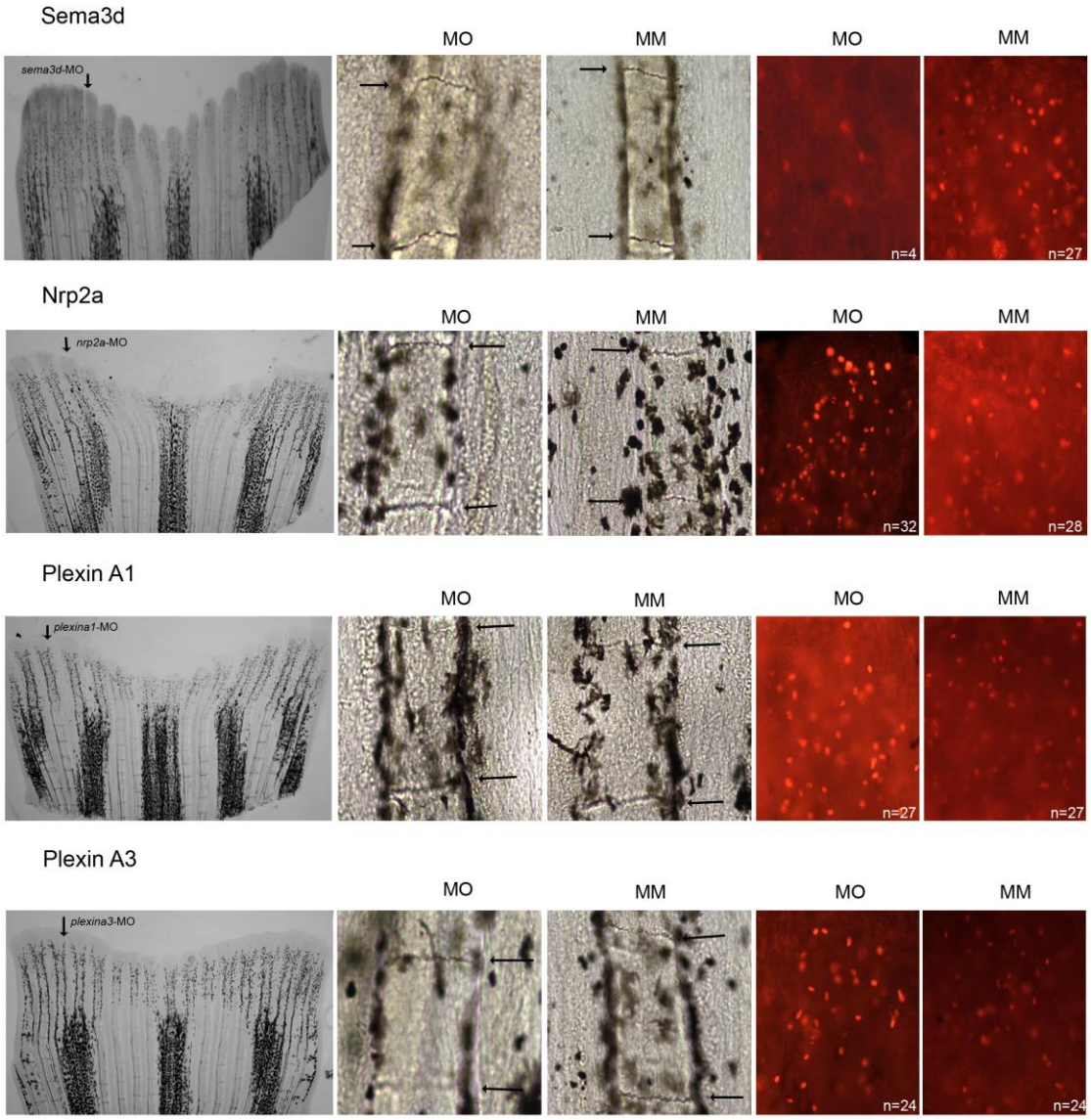

Figure 2.3 Representatives images of morpholino induced phenotypes. From left to right: representatives whole fins following injection in the dorsal most 5-6 fin rays (arrow); segment length in targeting morpholino injected (MO) and in 5 mis-match morpholino injected (MM); H3P positive cells in targeting morpholino injected (MO) and in 5 mis-match morpholino injected (MM).

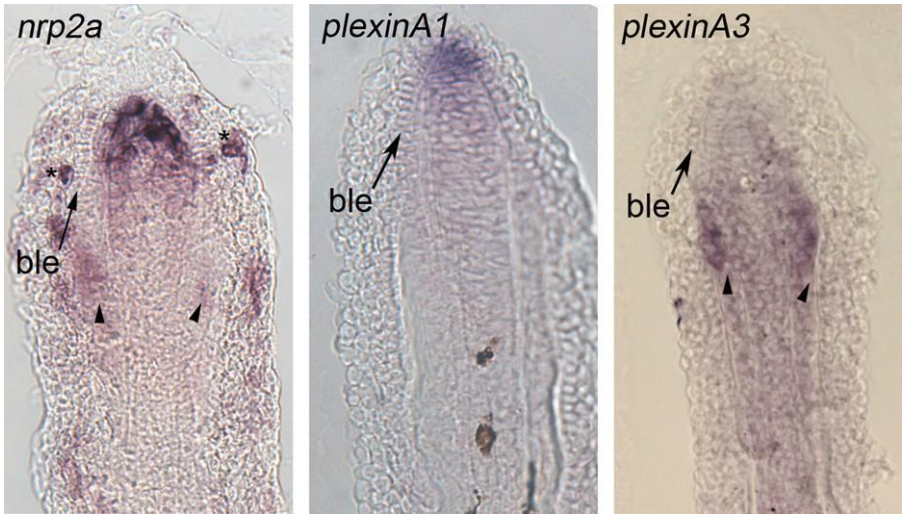

Figure 2.4 Gene expression of candidate receptors for Sema3d. Left: expression of *nrp2a* is primarily located in the distal blastema and in skeletal precursor cells. Staining of individual cells of the outer epithelial cells is also observed (*). Middle: expression of *plxna1* is primarily in the distal blastema and in the distal cells of the basal epidermis. Right: expression of *plxna3* is located in both the skeletal precursor cells and in the blastema. Arrows identify the basal layer of the epidermis (ble), arrowheads identify skeletal precursors.

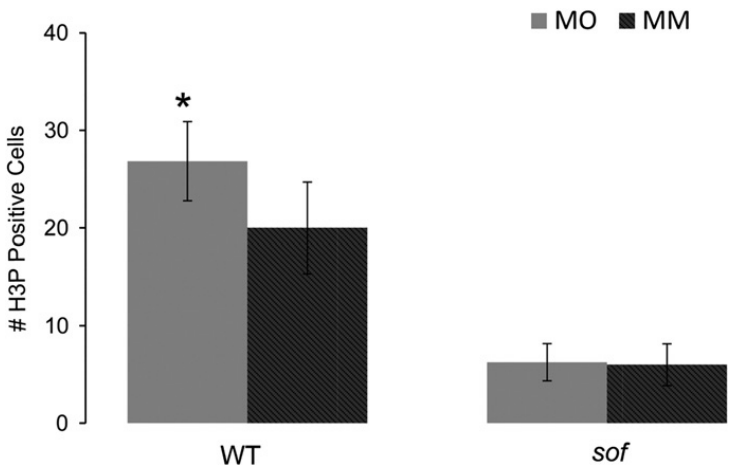

Figure 2.5 Nrp2a-knockdown effects are abrogated in *sof*^{b123}. Nrp2a-mediated gene knockdown causes an increase in cell proliferation when Sema3d is present at typical levels. In *sof*^{b123}, where *sema3d* expression is reduced, Nrp2a is unable to enhance the level of cell proliferation. MO, gene-targeting morpholino. MM, 5 mis-match/control morpholino.

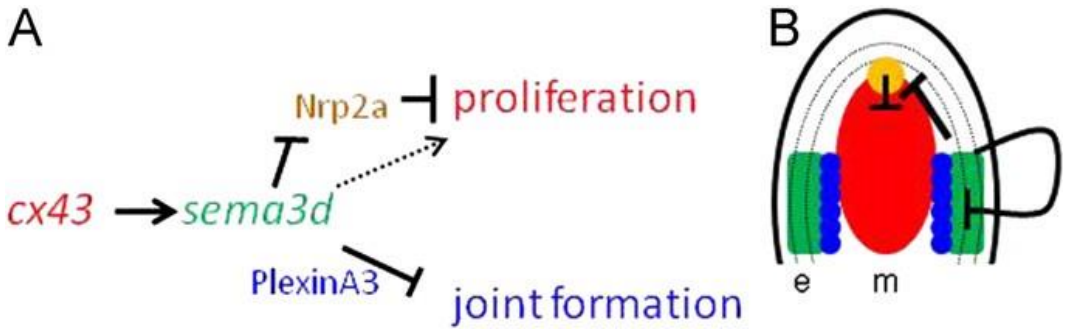

Figure 2.6 Model of how Cx43-Sema3d influences skeletal morphology. (A) Proposed pathway of Cx43-Sema3d and downstream receptors (text colors are coordinated with the cartoon in B). Cx43 activity in the dividing cells influences *sema3d* gene expression in the lateral skeletal precursors and basal layer of the epidermis. Secreted Sema3d promotes cell proliferation (dotted arrow) in the *cx43*-positive compartment by inhibiting a negative signal from Nrp2a in the distal blastema. Sema3d suppresses joint formation in the skeletal precursor cells by its interaction with PlxnA3, (B) cartoon illustrating the compartments of gene expression in the Cx43-Sema3d pathway (e, epithelium; m, mesenchyme; basal layer of the epidermis is dotted). The *cx43* mRNA is up-regulated in the blastema (red), adjacent to the *sema3d* -positive cells in the skeletal precursor cells and in the lateral basal layer of the epidermis (green). Cx43-dependent up-regulation of *sema3d* in the lateral compartment allows secreted Sema3d to signal back to the blastema via Nrp2a (yellow), relieving the Nrp2a inhibition of cell proliferation. Sema3d signaling via PlxnA3 in the skeletal precursor cells (blue circles) inhibits joint formation in the skeletal precursor cells, perhaps by influencing osteoblast/joint forming cell differentiation.

Gene	Primers for ISH	Morpholinos
sema3d	F-CGAAGTGTAGTACCATTTACG RT7-TAATACGACTCACTATAGGG- TATGAGGATCATATGTCC	MO-TGTCCGGCTCCCCTGCAGTCTTCAT 5MM-TGTGCCGCTGCCCTCCACTCTTCAT
nrp2a	F-CCAGTCCAGTAACCAGCG RT7-TAATACGACTCACTATAGGG- TCAAGCCTCGGAGCAGCAGC	MO-CCAGAAATCCATCTTTCCGAAATGT 5MM-CCACAAAACGATCTTTGCCAAATGT
plxna1	F-AAGTGTTCTCTGCGGCAG RT7-TAATACGACTCACTATAGGG- TTGCCCACCTCCGAAAAACC	MO-GCCACATATCTGCACTGGTCCTTGA 5MM-GCCAGATATGTGGACTGCTCCTTCA
plxna3	F-AGTGTCTCCTAAAGCAAC RT7-TAATACGACTCACTATAGGG- CCGCTTTCTGGAGCCTC	MO-ATACCAGCAGCCACAAGGACCTCAT 5MM-ATACGACCACCCAGAAGCACCTCAT

Table 2.1: Primer and morpholino sequences. The RNA polymerase T7 binding site is underlined in the reverse primers. MO = targeting morpholino; 5MM = control morpholino with 5 mismatch pairs to target sequence

Strain	Trial 1	Trial 2	Trial 3
Wild-type	1	1	1
sof^{b123}	0.6	0.65	0.71
alf^{dty86}	1.95	1.42	1.90
cx43-KD fins	0.7	0.4	0.55

The fold-difference with respect to wild-type is shown for each of three trials.

Table 2.2: Expression of *sema3d* via qRT-PCR

Mutant/ morphant	*cx43*	*sema3d*	Fin length	Segment length	Cell proliferation
sof^{b123}	low	low	short	short	reduced
alf^{dty86}	high	high	long	long	increased
cx43-KD	low	low	short	short	reduced
sema3d-KD	n/c	low	short	short	reduced
plxnA3-KD	n/d	n/d	short	short	n/c
nrp2a-KD	n/d	n/d	long	n/c	increased

Table 2.3: Phenotypes associated with altered expression of *cx43* and genes proposed to function downstream of Cx43. Changes in *cx43* and *sema3d* gene expression were evaluated by qRT-PCR. All knockdowns (KD) listed here were completed in wild type regenerating fins. No change (n/c); not done (n/d).

2.8 References

Berndt, J.D., Halloran, M.C., 2006. Semaphorin 3d promotes cell proliferation and neural crest cell development downstream of TCF in the zebrafish hindbrain. *Development*. 133, 3983–3992.

Borday, V., et al., 2001. *evx1* transcription in bony fin rays segment boundaries leads to a reiterated pattern during zebrafish fin development and regeneration. *Dev Dyn*. 220**,** 91-8.

Brown, A. M., et al., 2009. Osteoblast maturation occurs in overlapping proximal-distal compartments during fin regeneration in zebrafish. *Dev Dyn*. 238**,** 2922-8.

Flenniken, A. M., et al., 2005. A Gja1 missense mutation in a mouse model of oculodentodigital dysplasia. *Development*. 132**,** 4375-86.

Gomez, C., et al., 2005. Expression of Semaphorin-3A and its receptors in endochondral ossification: potential role in skeletal development and innervation. *Dev Dyn*. 234**,** 393-403.

Hoptak-Solga, A. D., et al., 2007. Zebrafish short fin mutations in *connexin43* lead to aberrant gap junctional intercellular communication. *FEBS Lett*. 581**,** 3297-302.

Hoptak-Solga, A. D., et al., 2008. Connexin43 (GJA1) is required in the population of dividing cells during fin regeneration. *Dev Biol*. 317**,** 541-8.

Iovine, M. K., et al., 2005. Mutations in *connexin43* (GJA1) perturb bone growth in zebrafish fins. *Dev Biol*. 278**,** 20819.

Iovine, M. K., Johnson, S. L., 2000. Genetic analysis of isometric growth control

mechanisms in the zebrafish caudal fin. *Genetics*. 155**,** 1321-9.

Kawasaki, Y., et al., 2007. Control of intracellular localization and function of Cx43 by SEMA3F. J. *Membrane Biology*. 217, 53-61.

Kolodkin, A. L., et al., 1992. Fasciclin IV: sequence, expression, and function during growth cone guidance in the grasshopper embryo. *Neuron*. 9**,** 831-45.

Lecanda, F., et al., 2000. Connexin43 deficiency causes delayed ossification, craniofacial abnormalities, and osteoblast dysfunction. *J Cell Biol*. 151**,** 931-44.

Lee, Y., et al., 2005. Fgf signaling instructs position- dependent growth rate during zebrafish fin regeneration. *Development*. 132**,** 5173-83.

Nechiporuk A., Keating MT., 2002. A proliferation gradient between proximal and msxb-expressing distal blastema directs zebrafish fin regeneration. *Development*. 129:2607-2617.

Paznekas, W. A., et al., 2003. Connexin 43 (GJA1) mutations cause the pleiotropic phenotype of oculodentodigital dysplasia. *Am J Hum Genet*. 72**,** 408-18.

Quint, E., et al., 2002. Bone patterning is altered in the regenerating zebrafish caudal fin after ectopic expression of *sonic hedgehog* and *bmp2b* or exposure to cyclopamine. *Proc Natl Acad Sci U S A*. 99**,** 8713-8.

Roth, L., et al., 2009. The many faces of semaphorins: from development to pathology. *Cell Mol Life Sci*. 66**,** 649-66.

Sims, K., et al., 2009. Connexin43 regulates joint location in zebrafish fins. *Dev Biol*. 327**,** 410-8.

Stains, J. P., et al., 2003. Gap junctional communication modulates gene transcription by altering the recruitment of Sp1 and Sp3 to connexin-response elements in osteoblast promoters. *J Biol Chem*. 278**,** 24377-87.

Thummel, R., et al., 2006. Inhibition of zebrafish fin regeneration using in vivo electroporation of morpholinos against *fgfr1* and *msxb*. *Dev Dyn*. 235**,** 336-46.

van Eeden, F. J., et al., 1996. Genetic analysis of fin formation in the zebrafish, Danio rerio. *Development*. 123**,** 255-62.

Wei, Y., et al., 1999. Phosphorylation of histone H3 is required for proper chromosome condensation and segregation. *Cell*. 97**,** 99-109.

Westerfield, M., 1993. The Zebrafish Book: A guide for the laboratory use of zebrafish (Brachydanio rerio). *University of Oregon Press,* Eugene, OR.

Wolman, M. A., et al., 2004. Repulsion and attraction of axons by *semaphorin3D* are mediated by different neuropilins in vivo. *J Neurosci*. 24**,** 8428-35.

Wolman, M. A., et al., 2007. Semaphorin3D regulates axon axon interactions by modulating levels of L1 cell adhesion molecule. *J Neurosci*. 27**,** 9653-63.

Yazdani, U., Terman, J. R., 2006. The semaphorins. *Genome Biol*. 7**,** 211.

Yu, H., et al., 2004. Cloning and embryonic expression of zebrafish neuropilin genes. *Gene Expr Patterns*. 4**,** 371-8.

Yu, H., Moens, C. B., 2005. Semaphorin signaling guides cranial neural crest cell migration in zebrafish. *Dev Biol*. 280**,** 373-85.

Zhou, Y., et al., 2008. Semaphorin signaling: progress made and promises ahead. *Trends Biochem Sci*. 33**,** 161-70

CHAPTER 3:

Identification of an *evx1*-dependent joint-formation pathway during fin regeneration

3.1 Abstract

Joints are essential for skeletal flexibly and form, yet the process underlying joint morphogenesis is poorly understood. Zebrafish caudal fins are comprised of numerous segmented bony fin rays, where growth occurs by the sequential addition of new segments and joints. Here, we evaluate joint gene expression during fin regeneration. First, we identify three genes that influence joint formation, *evx1*, *dlx5a*, and *mmp9*. We place these genes in a common molecular pathway by evaluating both their expression patterns along the distal-proximal axis (i.e. where the youngest tissue is always the most distal), and by evaluating changes in gene expression following gene knockdown. Prior studies from our lab indicate that the gap junction protein Cx43 suppresses joint formation. Remarkably, changes in Cx43 activity alter the expression of joint markers. For example, the reduced levels of *cx43* in the *sof* ^{b123} mutant causes short fin ray segments/premature joints. We also find that the expression of *evx1-dlx5a-mmp9* is shifted distally in *sof* ^{b123}, consistent with premature expression of these genes. In contrast, increased *cx43* in the *alf* ^{dty86} mutant leads to stochastic joint failure and stochastic loss of *evx1* expression. Indeed, reducing the level of *cx43* in *alf* ^{dty86} rescues both the *evx1* expression and joint formation. These results suggest that *cx43* influences the pattern of joint formation by influencing the timing of *evx1* expression.

3.2 Introduction

The precise location of joints provides both flexibility and form to the vertebrate skeleton. We use the zebrafish regenerating fin as a model to study skeletogenesis, including the appropriate formation of fin ray joints. Fin ray joints have been termed "fibrous joints" (Borday et al., 2001) since the articulation occurs in the bone matrix while the central mesenchyme remains continuous (Pacifici et al., 2006). These joints are distinct from synovial joints which completely articulate previously uninterrupted cartilaginous templates of the endochondral skeleton. The fin grows rapidly during regeneration, fully restoring fin size and pattern. The fin is comprised of multiple bony fin rays or lepidotrichia, and each fin ray is comprised of multiple bony segments separated by fin ray joints (or simply, joints). Each fin ray consists of two hemirays of bone matrix surrounding the mesenchyme, and several layers of epidermal cells surround the mesenchyme. Actinotrichia are bundles of collagen-like fibers that emanate from the distally located basal epidermal cells and serve as a substrate for osteoblasts to align and secrete bone matrix directly (Landis and Geraudie, 1990). The mesenchyme medial to the actinotricha includes dividing cells, undifferentiated cells, blood vessels, nerves, and connective tissues. The mesenchyme lateral to the actinotrichia includes the bone matrix, osteoblasts, and joint-forming cells. Joint-forming cells are a subpopulation of lateral mesenchymal cells that condense on the surface of the uninterrupted bone matrix and form an elongated row of cells at the site of the presumptive joint. These cells later separate into two rows of cuboidal cells that flank a newly established articulation in the bone matrix (Sims et al., 2009). Thus, these cells appear responsible for the articulation of the fin ray joints. We refer to the

osteoblasts and joint-forming cells collectively as skeletal precursor cells.

During growth and regeneration, the fin regenerates in the proximal to distal direction where new segments and new joints are continually added to the distal end of the fin ray. Thus, youngest tissue is always located more distally than mature tissue (Brown et al., 2009). Following amputation, the regenerate undergoes three main stages: wound healing, blastema formation, and outgrowth (Akimenko et al., 2003; Poss et al., 2003) The blastema is a specialized compartment comprised of rapidly proliferating cells, and is located in the distal and medial mesenchyme. These cells are the source of new tissue during regeneration. Recent studies show that several cell types in the regenerating fin are lineage restricted, meaning that new cells in the regenerating fin arise from precursor cells of the same cell type (Knopf et al., 2011; Singh et al. 2012; Sousa et al., 2011; Tu and Johnson, 2011). These cells undergo de-differentiation, cell proliferation, and re-differentiation, in order to replace lost tissue. This may not represent the only way to replace lost tissue, as others have found that osteoblasts are capable of de novo differentiation during fin regeneration (Singh et al.,2012). Osteoblasts and joint-forming cells appear to be derived from a common lineage (Tu and Johnson, 2011). To date, little is known about the genes required for differentiation of joint-forming cells, or indeed, the signals required to initiate this process.

The transcription factor Even-skipped 1 (Evx1) belongs to a family of vertebrate eve-related homeobox genes (Faiella et al., 1991). In zebrafish regenerating fins, the expression of *evx1* was observed strongly in the distal-most and youngest joints (Borday et al., 2001). Sections of *evx1* following *in situ* hybridization (ISH) showed a

strong expression level of *evx1* mRNA in the lateral compartment where skeletal precursor cells reside (Borday et al., 2001). More recently, *evx1* was shown to be required for joint formation since an *evx1* mutant fails to produce fin ray joints during regeneration (Schulte et al., 2011). Our evaluation of two other fin mutants, *short fin* (*sof* ^{b123}) and *another long fin* (*alf* ^{dty86}), suggest that the gap junction protein Connexin43 (Cx43) also contributes to joint formation. Both *cx43* mRNA and Cx43 protein are expressed throughout the medial mesenchyme, adjacent to the lateral populations of skeletal precursor cells (Hoptak-Solga et al., 2008). The *sof* ^{b123}mutant exhibits reduced levels of *cx43* mRNA and protein (without a lesion in the coding sequence) that lead to reduced cell proliferation, short segments (i.e. premature joints) and short fin length (Iovine et al., 2005). In contrast, the *alf* ^{dty86} mutant exhibits fin overgrowth and overlong segments on average due to stochastic joint failure (Sims et al., 2009). The *alf* ^{dty86} phenotype is not caused by mutations in *cx43* but coincidently has increased levels of *cx43* mRNA (van Eeden et al., 1996). We have shown that morpholino-mediated *cx43* knockdown in *alf* ^{dty86} rescues joint formation, suggesting that the higher levels of *cx43* in this mutant contributes to the loss of fin ray joints (Sims et al., 2009). Thus, reduced *cx43* leads to premature joints while increased *cx43* leads to joint failure. We interpret these findings to indicate that Cx43 suppresses joint formation, perhaps by communication between the medial *cx43*-positive mesenchyme and the lateral *evx1*-positive mesenchyme.

As an initial attempt to understand the events initiating and controlling joint formation, we first wished to define additional molecular players acting downstream of

evx1. Here, we describe the addition of two *evx1*-dependent joint gene markers that also contribute to joint formation: *distal-less homeobox-5a* (*dlx5a*) and *matrix-metalloproteinase-9* (*mmp9*). We also exploited the characteristics of low and high Cx43 activity in *sof* ^{b123} and *alf* ^{dty86} to address the relationship between the expression of these joint genes and Cx43 activity during joint patterning. We found that the onset of joint gene expression correlates with the level Cx43 activity. These results suggest that Cx43 may regulate joint formation by influencing the timing of *evx1* expression.

3.3 Materials and Methods

Statement on the ethical treatment of animals

This study was carried out in strict accordance with the recommendations in the Guide for the Care and Use of Laboratory Animals of the National Institutes of Health. The protocols used for this manuscript were approved by Lehigh's Institutional Animal Care and Use Committee (IACUC) (protocol identification #128, approved 11/14/2012). Lehigh University's Animal Welfare Assurance Number is A-3877-01. All experiments were performed to minimize pain and discomfort.

Fish maintenance

Zebrafish were derived from the C32 strain. Mutant fish used in these studies include *sof* ^{b123} (Iovine and Johnson, 2000) *alf* ^{dyt86} (van Eeden, et al., 1996) homozygous *evx1* $^{-/-}$ mutant fish, and heterozygous carriers (Schulte et al., 2011). All fish were raised and cared for at constant temperature of 25^{o}C in a 14 light: 10 dark photoperiod (Westerfield, 1993).

RNA probes and whole mount ISH

Antisense *evx1* probe was generated from 1µg of a PCR-generated linear template containing a T3 RNA polymerase binding site

F –TAATACGACTCACTATAG

R-T3 GGATCCATTAACCCTCACTAAAGGGAAGAGCTATGACGTCGCAT where the T3 binding site is underlined). Antisense digoxigenin-labeled *shh*, *lef1*, *mmp9*, and *dlx5a* probes were generated from *lef1* cDNA (Lee et al., 2009, *shh* cDNA (Lee et al., 2009) *mmp9* cDNA (Yoshinari et al., 2009) and *dlx5a* cDNA (Yoshinari et al., 2009).

The template for the *col10a1b* probe was a generous gift from the lab of Dr. David Parichy (gi68437010, located on chromosome 20).

Whole-mount ISH was performed on 5 dpa regenerating fins as described (Ton and Iovine, 2012). Stained fins were examined on a Nikon Eclipse 80i microscope. Images were collected using a digital Nikon camera. At least 4 regenerating fins were assessed at a time, and all markers were examined in triplicate.

ISH on cryo-sections

Fin regenerates (5dpa) were harvested and fixed overnight with 4% paraformaldehyde in PBS. Fins were dehydrated in 100% methanol at -20^{o}C. Next, fins were rehydrated in a methanol-PBS series of washes before embedding in 1.5% agarose/5% sucrose and equilibrated overnight in 30% sucrose. Blocks were mounted in OCT and cryosectioned (15 µm sections) using a Reichert–Jung 2800 Frigocut cryostat. Sections were collected on Superfrost Plus slides (Fisher) and allowed air dry overnight at room temperature. Slides may be stored in a freezer box at -20^{o}C for up to one year. For evaluation, two slides containing sections from two different fins were chosen. A marking pen (ImmEdge™ Pen H-4000; PAP pen, Vector Laboratories) was used to circle the sections. Probe was pre-hybridized with a mixture of 1X salt solution (NaCl, Tris HCl, Tris Base, $Na_2HPO4.7H_20$, NaH_2PO4, and 0.5 M EDTA) with 50% deionized formamide (Sigma), 10% dextran sulfate, 1mg/mL tRNA, and 1X Denhart's (Fisher) at 70^{o}C for 5 mins. Hybridization with digoxigenin-labeled antisense probes was completed overnight at 65^{o}C. The next day, slides underwent series of washes in a

solution that has 1X SSC, 50% formamide and 0.1% Tween-20 at 65^{o}C. Slides were then transferred to room temperature for extensive washes in MABT (100 mM Maleic acid, 150 mM NaCl, and 0.1% Tween-20) before incubation in blocking solution (MABT, Goat serum and 10% milk) for at least 2 hours or overnight. Anti-digoxigenin Fab fragments (pre-absorbed against zebrafish tissue) were used at 1:5000 overnight at 4^{o}C. After incubation, slides were washed in MABT four times followed by two short washes in staining buffer (100mM Tris, 9.5, 50 mM MgCl2, 100mM NaCl, and 0.1% Tween20). Slides were next transferred to 10% polyvinyl alcohol (PVA; MW: 86,000) staining solution plus NBT/BCIP stock solution (Roche) and development proceeded overnight at 37^{o}C. Once observing purple staining on the sections, the reaction was stopped by washing the slides with PBST for at least 3 hours. Sections were mounted in 100% glycerol and examined on a Nikon Eclipse 80i microscope. Images were collected using a digital Nikon camera.

Morpholino-mediated gene knockdown and electroporation

Injection and electroporation experiments were performed as described previously (Hoptak-Solga et al., 2008; Sims et al., 2009; Ton and Iovine, 2012; Thummel et al., 2006). Targeting morpholinos were designed against the start codon and modified with fluorescein at the 3' end (Gene Tools, LLC) to provide a charge and for detection. Control morpholinos were either custom mismatch morpholinos containing five mismatches to the targeted gene or were the Gene Tools 'standard control' morpholino, which does not recognize any zebrafish genes. Following injection and electroporation, fins were harvested at 1day post electroporation (dpe) to evaluate changes in gene

expression. At least 4 regenerating fins were treated per morpholino (targeting or control), and all knockdown experiments were completed in triplicate.

Morpholino sequences for *cx43* were described previously (Hoptak-Solga et al., 2008). Morpholinos used here include: *evx1*-MO, CTTTCCGTGCTTCGGCGAGCCCATT; *evx1*-MM, CTTTGCCTGGTTCGGCCACCCCATT; *mmp9*-MO, AAACGCCAGGACTCCAAGTCTCAT; *dlx5a*-MO (also used in Talbot et al., 2010), CGAATACTCCAGTCATAGTTTGGAT; Standard control MO, CCTCTTACCTCAGTTACAATTTTATA.

Measurements

Measurements of the distal boundaries of ISH expression domains to the distal end of the fin were taken from the third fin ray (V+3) since that was established as a standard (Iovine and Johnson, 2000). Student's t-tests were performed to determine if data sets were statistically different ($p < 0.05$). At least 8 fin rays per marker (*evx1*, *dlx5a*, *mmp9, col10a1b*, *shh*, and *lef1*) were measured.

Quantitative real-time PCR

For qRT-PCR analysis, TRIZOL RNA extraction was made from the 5 dpa regenerating fins of *evx1*$^{-/-}$, *evx1*$^{+/-}$, or 1 dpe for *dlx5a*-morpholino injected fins (targeting or standard morpholino). A minimum of 8 fins was used for total RNA extraction. For each sample, 1 µg of total RNA were reverse transcribed with SuperScript III reverse transcriptase (Invitrogen) using oligo-dT primers. Primers for qPCR analysis of *dlx5a* (GAGCCCGCAAGAAAAAGAAA; CCGTTGACCATCCTTACTTCG), *mmp9* (CGTGACGTTTCCTGGAGATGT; TCATCCGCTAGCTGTGTGTTG), *and col10a1b*

(ATCCCACACTGTTGCTGGTGA; CCGTTCTTTCCAGGACTTCCA), were designed using Primer express software. Two independent RNA samples were used for the experimental comparison and qPCR for each gene was done in duplicate. The samples were analyzed using Rotor-Gene 6000 series software (Corbette Research) and the average cycle number (C_T) was determined for each amplicon. Delta C_T (ΔC_T) values represent normalized expression levels of the test with respect to *actin*, the internal control. The relative level of gene expression between experimental and control samples, which is the fold difference (i.e. either between *evx1*$^{-/-}$ and *evx1*$^{+/-}$, or between targeting and control morpholino-treated fins), was determined using the delta delta C_T ($\Delta\Delta C_T$) method (i.e., $2^{-\Delta\Delta CT}$).

3.4 Results and Discussion

dlx5a and *mmp9* are expressed downstream of *evx1*

Since our studies suggest that Cx43 influences joint formation, we were interested in identifying additional genes that function together to regulate this process. Unlike osteoblast genes which are expressed in broad domains throughout the lateral compartment in the regenerating fin (Brown et al., 2009) genes expressed during joint formation tend to be expressed in a discrete group of cells. The expression pattern typically appears as a band of cells following whole mount ISH, and these cells are located within the lateral population of skeletal precursor cells (i.e. see Borday et al., 2001). Thus, we identified *evx1*, *dlx5a*, *mmp9*, and *col10a1b* as candidate joint genes based on their location of expression (Borday et al., 2001; Yoshinari et al., 2009; Dr. Parichy generous gift. The *col10a1b* sequence appears to be a paralog of *col10a1a* located on chromosome 17). We first confirmed the location of gene expression of this set of genes using whole mount ISH on 5 days-post-amputation (dpa) regenerating fins and by ISH on cryo-sectioned tissue of 5 dpa caudal fins. As expected, we found *evx1*, *dlx5a*, *mmp9* and *col10a1b* are strongly expressed in a discrete group of cells in the lateral compartment where the skeletal precursor cells reside (Figure 3.1).

It has been proposed that *evx1* is one of the earliest joint gene markers (Borday et al., 2001). Indeed, *evx1*$^{-/-}$mutants lack fin ray joints, demonstrating that *evx1* is required for joint formation (Schulte et al., 2011). We have also found that morpholino-mediated knockdown of *evx1* is sufficient to cause joint failure (data not shown). We next investigated if expression of *dlx5a*, *mmp9*, and *col10a1b* depend

upon *evx1* for their expression by taking advantage of both morpholino-mediated knockdown of *evx1* and the *evx1*$^{-/-}$ mutant fins. We expected to find that expression of *evx1*-dependent genes is reduced in the knockdown fins and completely absent in the *evx1*$^{-/-}$ mutant fins. Indeed, we found that expression signals of *dlx5a* and *mmp9* are reduced in *evx1*-knockdown fins, while *col10a1b* expression appeared unaffected (Figure 3.2). One possibility for failure to observe a knockdown effect on *col10a1b* expression is that the morpholino did not target the *col10a1b*-expressing cells located in the lateral mesenchyme. Unfortunately, it was not possible to evaluate doubly-labeled cell for the morpholino (flourescein-tagged) and for gene expression since the fluorescein signal is labile following in situ hybridization (Figure 3.3). However, we regularly observe that our morpholinos target all compartments of the regenerating fin, including the lateral compartment of skeletal precursor cells (Figure 3.3). We next evaluated gene expression in *evx1*$^{-/-}$ regenerating fins. Similar to our findings using the *evx1*-morpholino, we find that expression of *dlx5a* and *mmp9* are more severely reduced in *evx1*$^{-/-}$regenerating fins, while *col10a1b* is also not affected in those fins (Figure 3.2). Interestingly, *dlx5a* and *mmp9* are not completely abolished in the *evx1*$^{-/-}$ mutants, suggesting that an alternate, non-*evx1*- dependent pathway may also contribute to expression of these genes. These findings were confirmed by quantitative RT-PCR (qRT-PCR). We calculated the fold-difference for each gene between *evx1*$^{-/-}$ and *evx1*$^{+/-}$ regenerating fins. We find that *dlx5a* and *mmp9* expression is reduced (i.e. fold-change less than 1) but not abolished in *evx1*$^{-/-}$ regenerating fins. Furthermore, expression of *col10a1b* was not influenced by the loss of *evx1* (Figure 3.4). Taken

together, these data suggest that *dlx5a* and *mmp9* are expressed downstream of *evx1*, while *col10a1b* is not. Continued studies therefore focused on *dlx5a* and *mmp9*. Both *evx1* and *dlx5a* encode for homeobox domain- containing transcription factors, although their direct targets are largely unknown. The *mmp9* gene codes for a matrix metalloprotease enzyme, which is responsible for degradation of extracellular matrix proteins. During the process of joint morphogenesis, the previously uninterrupted bone matrix separates into two bony elements (Sims et al., 2009). It is possible that Mmp9 activity contributes to this articulation event through digestion of the bone matrix.

We next wished to distinguish between the *dlx5a* and *mmp9* genes acting simply as either joint markers, or as providing a function during joint formation. Reduced function of genes required for joint formation is predicted to cause either complete joint failure or a delay of joint formation (i.e. longer segments). We find that morpholino-mediated knockdown of *dlx5a* and *mmp9* both cause increased segment length (Figure 3.5). Importantly, the knockdown of these genes represents the first example of a manipulation causing longer segments in the fin. Indeed, the only other example of long fin ray segments is the *alf* ^{dty86} mutant. We cannot rule out the possibility that *dlx5a* and *mmp9* may also influence the rate of fin growth. However, changes in growth rate are not sufficient to influence segment length. Fish grown in crowded conditions grow slower than fish grown in sparse conditions, but segment length is not different between these groups (Iovine and Johnson 2000). Moreover, abrogation of either Fgfr1 or Shh, while influencing the rate of cell proliferation and fin length, do not influence segment length Thus, these findings support a model where *dlx5a* and *mmp9* contribute

to correct joint placement, irrespective of any putative role in regulating fin growth.

Placing the genes of the joint pathway in a linear order

Previously, our lab showed that the early genes required for osteoblast differentiation initiated in the more distal, less mature osteoblasts, while onset of expression of late osteoblast genes was observed in the more proximal, more mature osteoblasts (Brown et al., 2009). Here we applied a similar approach for this set of joint-forming genes in an attempt to reveal a preliminary order of the *evx1*-dependent genes. We completed whole mount ISH at 5 dpa and measured the distance of expression domains of *evx1*, *dlx5a*, and *mmp9* to the distal end of the fin. As anticipated, *evx1* is expressed in the most distal domain of skeletal precursor cells, consistent with this gene acting the earliest (Figure 3.6). Since *dlx5a* and *mmp9* appear downstream of *evx1*, we expected to find their gene expression more proximally. We find that *dlx5a* is expressed more proximally than *evx1*, while *mmp9* is expressed more proximally than both *evx1* and *dlx5a* (Figure 3.6). These findings support the hypothesis that *dlx5a* and *mmp9* are expressed downstream of *evx1* and further suggests the following linear pathway: *evx1* followed by *dlx5a* followed by *mmp9*.

To confirm this predicted order of gene expression, we examined changes in gene expression following *dlx5a*-knockdown and *mmp9*-knockdown by whole-mount ISH (Figure 3.7). We found that *mmp9* expression is reduced in fins treated for *dlx5a*-knockdown, consistent with the hypothesis that *mmp9* is expressed downstream of *dlx5a*. This reduction of *mmp9* expression in *dlx5a*-knockdown fins was confirmed by qRT-PCR. We calculated the fold-difference for *mmp9* expression in *dlx5a*-knockdown fins

compared with control knockdown fins. We find that *mmp9* levels are reduced approximately 40% (i.e. fold-change of 0.54 and 0.57 from independent RNA samples). In contrast, *dlx5a* expression is not affected by *mmp9*- knockdown. Similarly, *evx1* expression is not affected by either *dlx5a*-knockdown or by *mmp9*- knockdown. Together with our earlier findings that loss of *evx1* causes reduced expression of *dlx5a* and *mmp9* (i.e. Figure 3.2), these results confirm the relative order of gene expression predicted by the expression patterns along the proximal-distal axis and further suggests that *dlx5a* and *mmp9* function does not feedback on expression of *evx1*.

Cx43 regulates the evx1-dependent joint pathway

Based on our previous findings, we have suggested that Cx43 activity in the medial compartment, adjacent to the population of skeletal precursor cells, suppresses joint formation (Sims et al., 2009). For example, the *sof* ^{b123} mutant (reduced *cx43*) exhibits short segments/premature joints. Therefore, we predicted that the expression of the joint genes would initiate sooner, or more distally, in *sof* ^{b123} fins than in wild type. Indeed, expression of *evx1*, *dlx5a*, and *mmp9* genes are each initiated more distally in *sof* ^{b123} regenerating fins compared with wild type (Table 3.1). These findings are consistent with the reduced level of Cx43 activity causing premature activation of the *evx1*-dependent joint pathway, and premature joints. It may be suggested that the reduced growth rate of *sof* ^{b123} causes the shift of gene expression domains to more distal locations. However, such a shift in patterning due to differential growth rates has not been observed. For example, fin amputations at more proximal locations regenerate more rapidly than fin amputations at more distal locations. However, when comparing

these conditions for four different genes located in the basal layer of the epidermis (i.e. *lef1, shh, wnt5b, pea3*), the distance of expression of the gene domain to the distal end did not appear altered, although the strength of expression and/or size of the expression domain can change (Lee et al., 2009). Therefore, to confirm that the reduced growth rate of *sof* ^{b123} does not influence the patterning of gene expression in general, we compared the expression of both *shh* and *lef1* between *sof* ^{b123} and wild-type regenerating fins. Importantly, we found no significant changes in the distance of the distal expression domains for either gene to the distal end of the fin between wild type and *sof* ^{b123} (although we do see that overall expression levels are slightly reduced) (Figure 3.8). Thus, the reduced growth rate of *sof* ^{b123} is likely not the cause of the distal shift in joint gene expression. Rather, we suggest that reduced *cx43* in *sof* ^{b123} leads to premature expression of the joint genes.

We next examined joint gene expression in the *alf* ^{dty86} mutants, which exhibit stochastic joint failure and overlong segments on average due to increased expression levels of *cx43* (van Eeden et al., 1996; Sims et al., 2009). Thus, in *alf* ^{dty86} we expected to observe an irregular pattern (on/off) of joint gene expression and/or more proximal expression of the joint genes compared with wild type. Indeed, *evx1* is expressed in a stochastic pattern and also initiates more proximally (Figure 3.9 and Table 3.1). Since *evx1* is required for joint formation (Schulte et al., 2011) these findings suggest that the stochastic nature of *evx1* expression is the underlying cause of stochastic joint failure in *alf* ^{dty86}. Moreover, we suggest that the increased level of *cx43* in *alf* ^{dty86} is the underlying cause of stochastic *evx1* expression (i.e. since *cx43*-knockdown rescues joint

formation in *alf* ^{dty86}, Sims et al., 2009). Therefore, we next wished to determine if *cx43*-knockdown rescues *evx1* expression. We tested this by injecting either a *cx43*-targeting morpholino or a *cx43*- mismatch morpholino across all fin rays in *alf* ^{dty86} regenerating fins. Next, the percentage of *evx1*-positive fin rays was determined for each fin. We find that *cx43*-knockdown in *alf* ^{dty86} regenerating fins significantly increases the percentage of *evx1*-positive fin rays compared with the *cx43*-mismatch morpholino and compared with uninjected *alf* ^{dty86} regenerating fins (Figure 3.10). These findings reveal that *cx43*-knockdown relieves the suppression of *evx1* expression, thereby permitting joint formation. Therefore, we suggest that *cx43* suppresses joint formation by suppressing *evx1* expression. Previously, we found that Cx43 regulates joint formation via *sema3d-plxna3*. To test whether *cx43* suppression function through the *sema3d-plxna3*, we injected *plxna3*-targeting morpholino or a *plxna3*- mismatch morpholino across all fin rays in *alf* ^{dty86} regenerating fins then calculated the percentage of *evx1*-positive fin rays. We find that indeed *plxna3*-knockdown rescues *evx1* expression. In contrast, knockdown of *nrp2a* (the putative receptor of Sema3d that belongs to the cell proliferation pathway) does not (Figure 3.10). These findings strongly suggest that the previous identified pathway (*sema3d-plxna3*) downstream of *cx43* regulates joint formation through the suppression of *evx1* expression.

It was anticipated that the stochastic nature of *evx1* expression would lead to stochastic expression of both *dlx5a* and *mmp9*. However, this was not observed (Figure 3.9). Instead, we find their expression is activated in all fin rays in *alf* ^{dty86}, consistent with the observation that *dlx5a* and *mmp9* expression are not completely

eliminated in the *evx1*$^{-/-}$ mutant, and therefore appear to be activated even in the absence of *evx1*. Since joint failure occurs despite expression of *dlx5a* and *mmp9*, these data also suggest that *dlx5a* and *mmp9* cannot mediate joint formation without the additional expression of *evx1*. Thus, since *evx1* is required for joint formation but *dlx5a* and *mmp9* are required but not sufficient for joint formation, *evx1* must activate at least one other pathway to establish fin ray joints. Continued studies are required to identify this pathway.

Model of joint differentiation during fin regeneration

Our analyses of joint gene expression suggest a model for joint formation that requires *evx1*, which is expressed the earliest, followed by expression of *dlx5a* and *mmp9* (Figure 3.11). Each of these genes is expressed in the population of skeletal precursor cells, adjacent to the Cx43-positive medial mesenchyme, and all three genes contribute to joint formation. We further suggest that Cx43 influences joint formation by influencing *evx1* expression. When *cx43* activity is reduced, as in *sof*^{b123}, expression of all *evx1*-dependent joint genes is shifted distally, consistent with the observation that *sof*^{b123} produces premature joints. When *cx43* activity is increased, as in *alf*^{dty86}, expression of *evx1* is irregular, consistent with the stochastic joint failure observed in *alf*^{dty86} regenerating fins. Indeed, *cx43*-knockdown rescues both *evx1* expression and joint formation (Sims et al., 2009) in *alf*^{dty86}. Interestingly, expression of *dlx5a* and *mmp9* are not randomized, but instead are consistently expressed in all fin rays. Continued studies will be necessary to identify additional possible *evx1*-dependent pathways, and to understand how *dlx5a* and *mmp9* expression is

maintained in the absence of *evx1*.

3.5 Figures

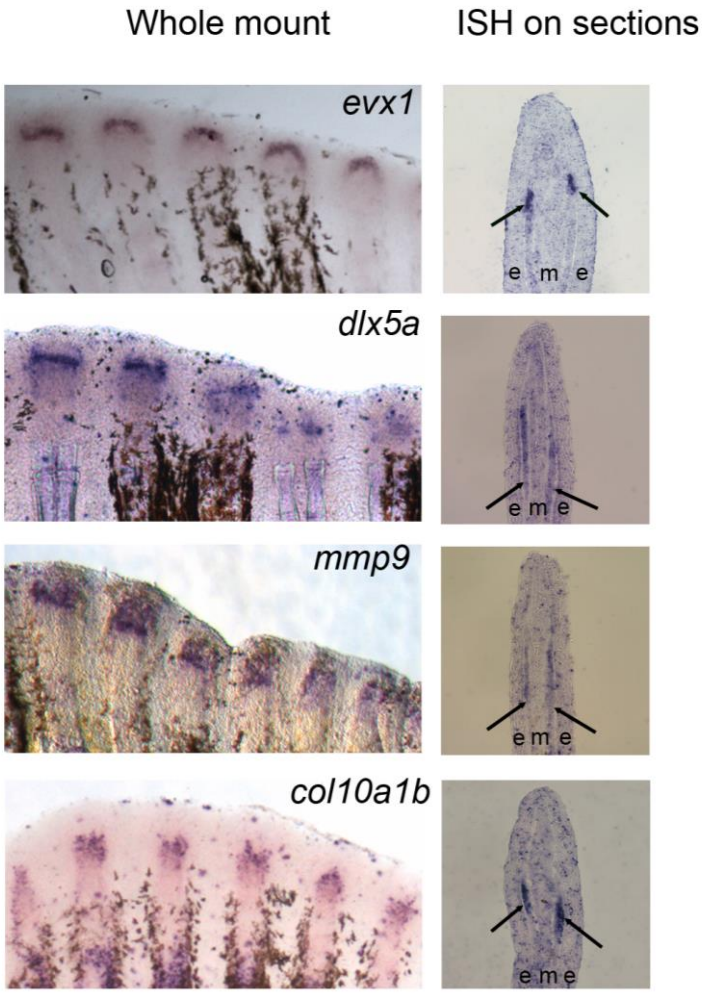

Figure 3.1 Expression of joint genes in regenerating fins. (Left) Whole mount ISH shows *evx1*, *dlx5a*, *mmp9*, and *col10a1b* are expressed in 5 dpa wild type fins. (Right) ISH on wild-type 5 dpa cryosections reveal expression of joint genes in the lateral skeletal precursor cells. Arrows point to gene expression in the skeletal precursor compartment. (e) epithelium; (m) mesenchyme

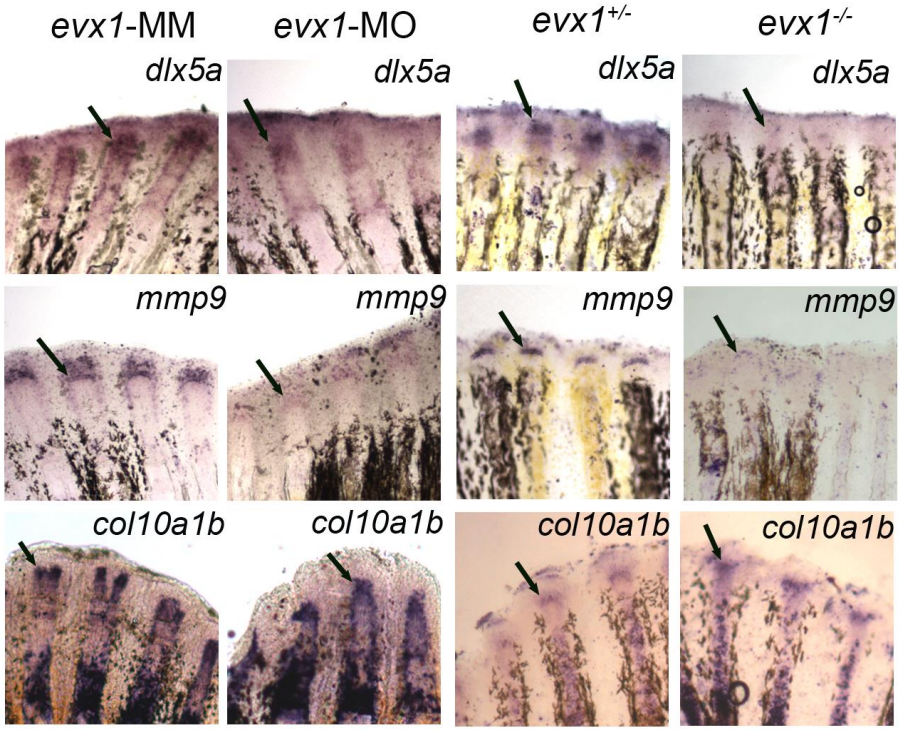

Figure 3.2 *dlx5a* and *mmp9* are genes downstream of *evx1*. (A) Whole mount ISH shows levels of *dlx5a* expression and *mmp9* expression are reduced in the *evx1*-morpholino (*evx1*-MO) injected side compared with the *evx1*-mismatch (*evx1*-MM) injected side, while the level of *col10a1b* expression is unchanged. (B) Whole mount ISH on *evx1*$^{-/-}$ mutants displays similar results seen in the *evx1*-MO injected fins, except that a stronger reduction in *dlx5a* and *mmp9* is observed. Arrows identify regions of the fin where staining is present and/or expected (i.e. in the cases where reduced *evx1* influences expression levels).

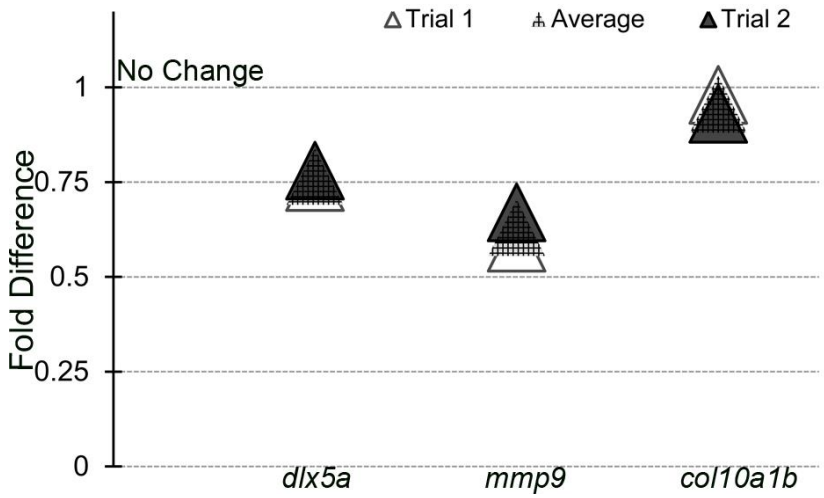

Figure 3.3 Quantitative RT-PCR confirms changes in gene expression downstream of *evx1*. The fold difference of expression between *evx1*$^{-/-}$ and *evx1*$^{+/-}$ regenerating fins was determined for *dlx5a*, *mmp9,* and *col10a1b*. A fold-difference of 1 indicates no difference between these samples. Both *dlx5a* and *mmp9* expression levels are reduced in *evx1*$^{-/-}$, while the expression level of *col10a1b* was not. Two independent cDNA samples from 5 dpa regenerating fins were prepared. Each trial represents the average results from one cDNA sample examined in duplicate. The average represents the average results from both trials.

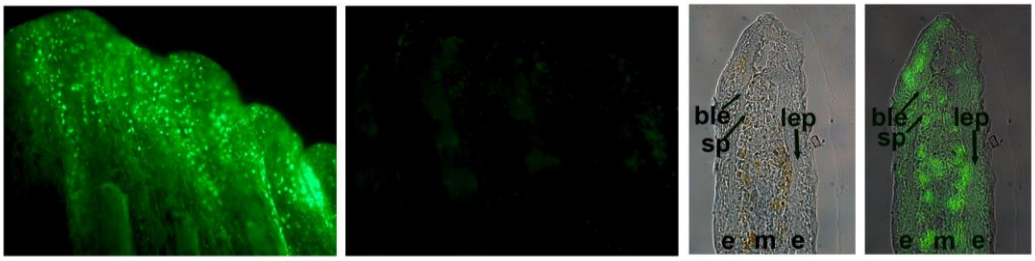

Figure 3.4 Morpholinos target all cellular compartments of the regenerating fin. The two left panels demonstrate loss of fluorescein signal of the tagged morpholino following in situ hybridization. The two right panels demonstrate that 24 hours post morpholino injection/electroporation, fluorescein-positive cells are observed in all cellular compartments in freshly harvested fins. The basal layer of the epidermis (ble) is identified. The skeletal precursor cells (sp) are located adjacent to the ble. Morpholino uptake, identified as green fluorescent cells, is observed in the outer epithelial layers, in the skeletal precursors, and in the medial mesenchyme.

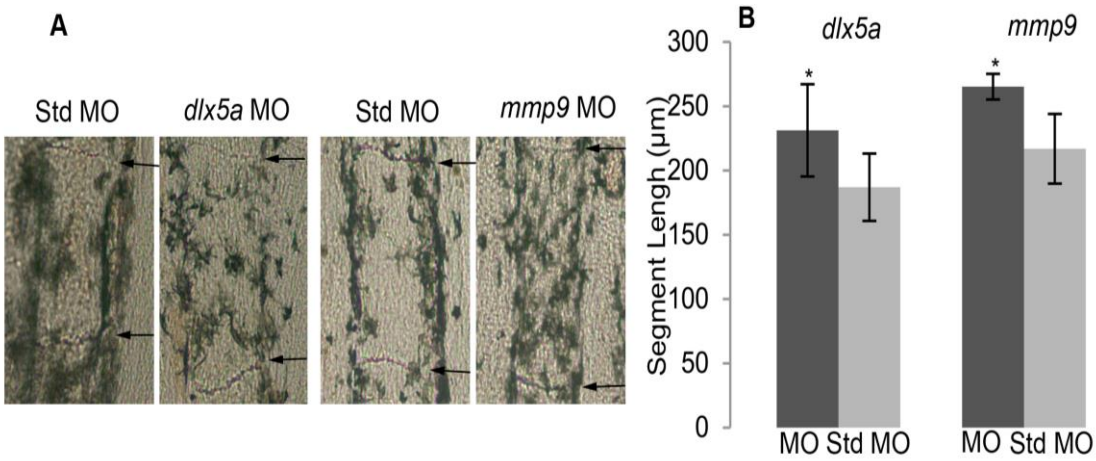

Figure 3.5 *dlx5a* and *mmp9* are necessary for correct joint placement. (A) Segment length is increased following targeted gene knockdown of *dlx5a* and *mmp9* compared with standard control (std) morpholino knockdown (negative control). (B) Segment length is increased in *dlx5a*-knockdown and *mmp9*-knockdown fins compared with standard control morpholino. Statistically different data sets (*) were determined by the student's t-test where $p<0.05$. The p-value for the comparison of segment length for the dlx5a-treated fins was $p = 0.0047$. The p-value for the comparison of segment length for the mmp9-treated fins was $p = 0.0018$. Error bar represent the standard deviation. MO, morpholino.

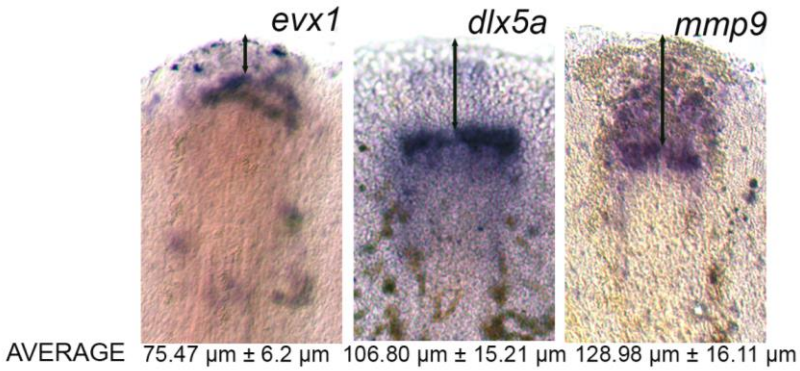

Figure 3.6: Expression domains of joint genes expressed during fin regeneration. The double arrow identifies the measured distance between the expression domains and the distal top of the fin. The measurement was taken from the third ray of each fin and was calculated in average and in standard deviation (±).

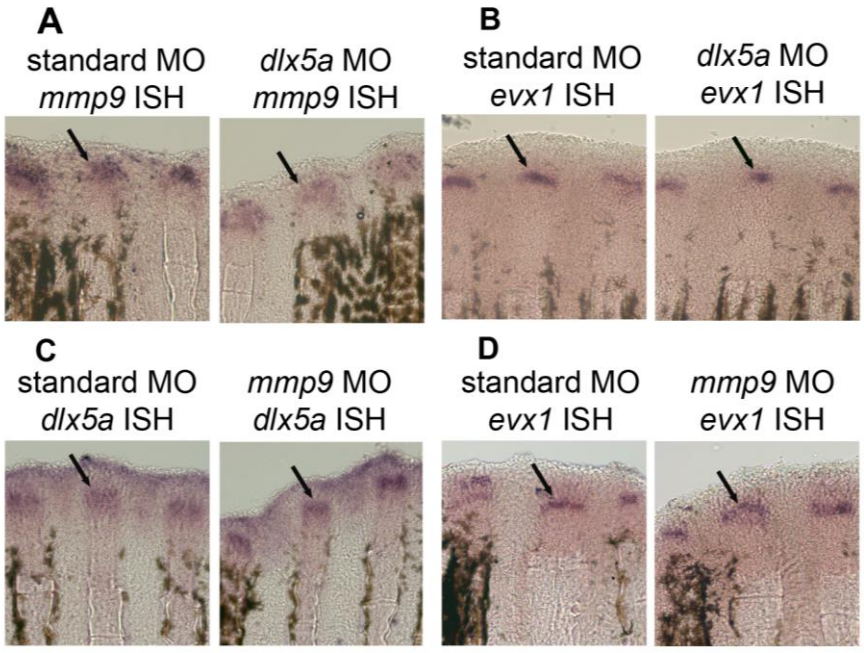

Figure 3.7 Confirmation of the predicted *evx1*-dependent joint pathway. Morpholino mediated gene knockdown followed by whole mount ISH show that *dlx5a*-knockdown causes reduced *mmp9* expression (A) but does not influence *evx1* expression (B) *mmp9*-knockdown does not influence *dlx5a* expression (C) or *evx1* expression (D). Arrows point to the in situ hybridization staining.

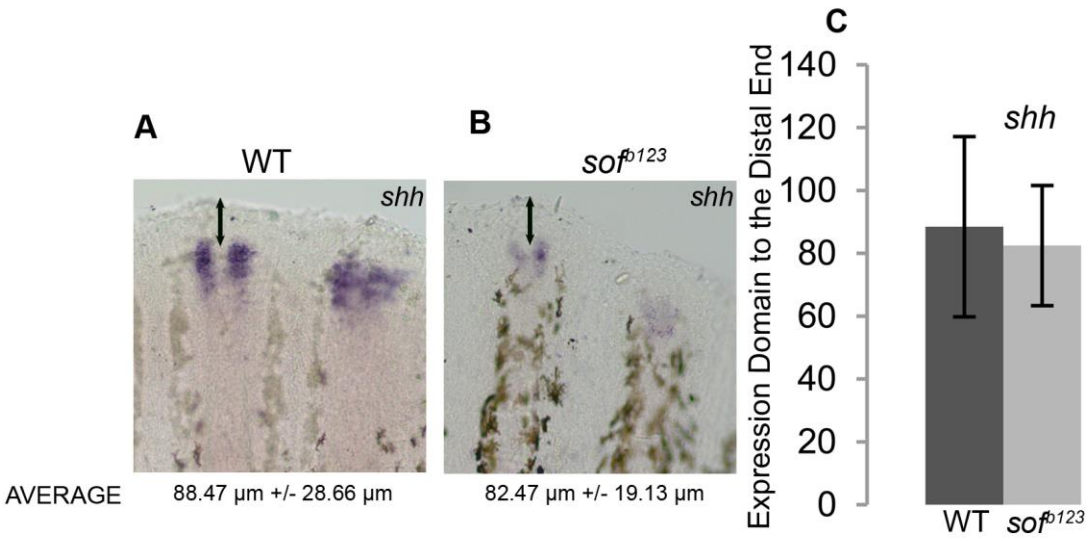

Figure 3.8 Reduced growth rate of *sof* ^{b123} mutants does not influence patterning of gene expression. (A) Whole mount ISH of *shh* on WT fins (A) and on *sof* ^{b123} fins (B). (C) The distance of expression of *shh* and *lef1* to the distal end of the fin is not influenced by the reduced growth rate of *sof* ^{b123} since the distances of the expression domains for *shh* and *lef1* are not statistically different by the student's t-test ($p>0.05$). The p-value for comparison of the *shh* domain was $p = 0.19$. The p-value for the comparison of the *lef1* domain was $p = 0.30$. Arrows identify the region of the fin that was measured, from the distal expression domain to the distal end of the fin. Error bars represent the standard deviation.

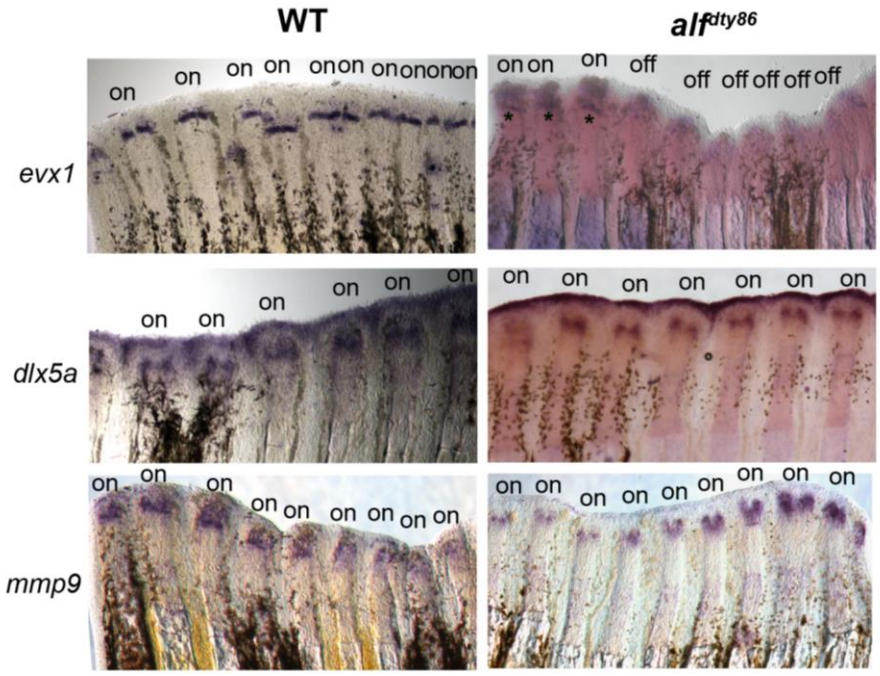

Figure 3.9 Expression of joint genes in *alf* ^{dty86}. Whole mount ISH of *evx1* shows that *evx1* is expressed consistently in wild-type but irregularly in *alf* ^{dty86} (i.e. "on" vs. "off") Asterisks were placed just proximal to the *evx1*-positive rays in *alf* ^{dty86}, which are present even though expression is weak. In contrast, *dlx5a* and *mmp9* appear to be expressed in all fin rays in both wild-type and *alf* ^{dty86} fins.

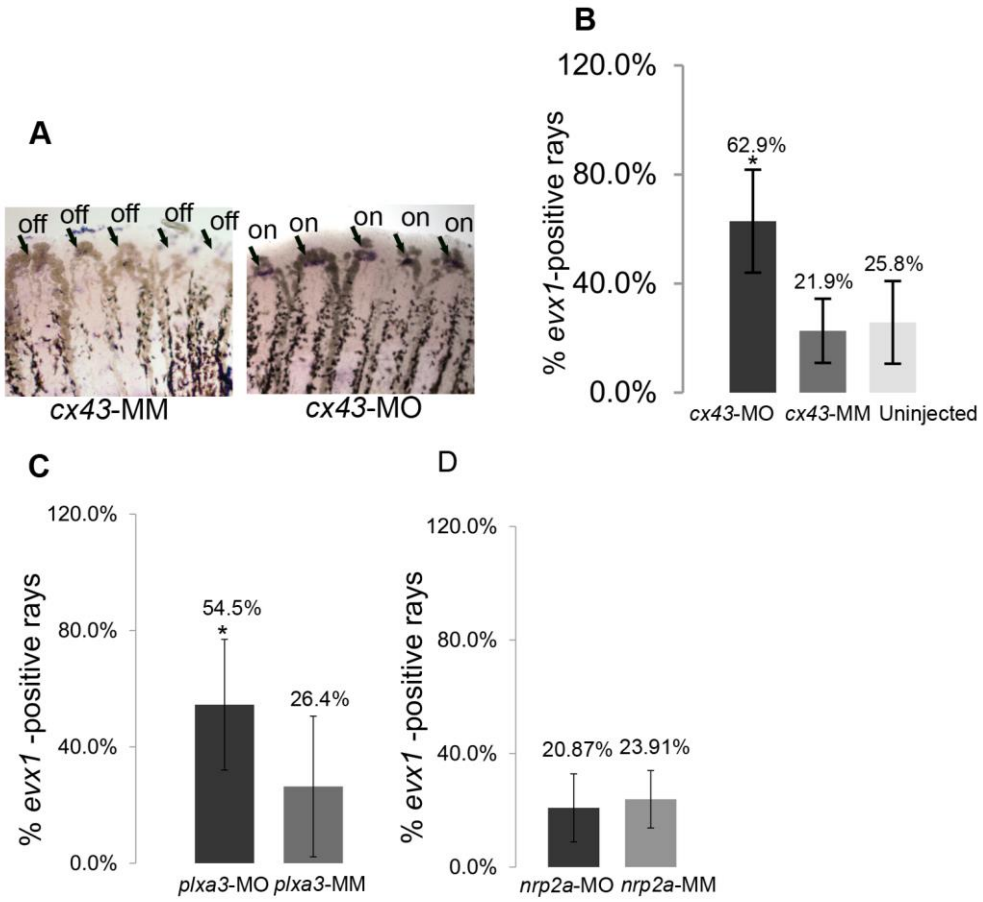

Figure 3.10 Knockdown of *cx43* and *plxna3* rescue *evx1* expression in *alf*^{dty86}. (A) Whole mount ISH of *evx1*shows that *evx1* is expressed in most fin rays in *cx43*-morpholino (MO) fins (on) but not in *cx43*-mismatch (MM) fins (off). Arrow identify *evx1*-positive signal. (B) *evx1* expression is present in a much higher percentage of fin rays in *alf*^{dty86} following injection/electroporation of *cx43*-MO compared with either the *cx43*-MM control fins or the uninjected fin rays. (C) *evx1* expression is present in a much higher percentage of fin rays following *plxa3*-MO compared with *plxna3*-MM control fin rays. (D) There is no significant difference in *evx1* rescue between *nrp2a*-MO and *nrp2a*-MM control. Statistical significance (*) was determined by student's t-test where $p<0.05$ show significant differences. The p-value for the comparison of *cx43*-MO and *cx43*-MM was $p = 0.0015$. The p-value for the comparison of *cx43*-MO and uninjected fin rays was $p = 0.0036$. The p-value for the comparison of *plxna3*-MO and *plxna3*-MM was 0.00052. The p-value for the comparison of *nrp2a*-MO and *nrp2a*-MM was 0.72. The bars represent the standard deviation.

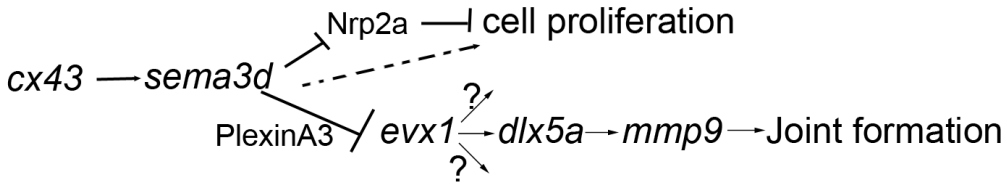

Figure 3.11 Model of the identified joint pathway. Both *dlx5a* and *mmp9* appear to be regulated by both *evx1*-dependent and non-*evx1*-dependent manners. In addition, *evx1* may activate additional genes required for joint formation. Cx43 utilizes Sema3d signaling pathway to suppress joint formation (via PlexinA3 receptor but not via Nrp2a receptor) by influencing *evx1* expression.

	WT	*sof*^{b123}	*alf*^{dty86}
evx1	(+) 75.47 µm ± 6.2 µm N=9	(+) 64.1 µm ± 4.36 µm N=9	(+/-) 109.33 µm ± 20.7 µm N=9
dlx5a	(+) 106.80 µm ± 15.21 µm N=8	(+) 79.16 µm ± 10.26 µm N=8	(+) 110.52 µm ± 22.15 µm N=15
mmp9	(+) 128.98 µm ± 16.11 µm N=8	(+) 86.34 µm ± 14.65 µm N=8	(+) 110.73 µm ± 19.55 µm N=15

Table 3.1: Expression domains of genes contributing to joint formation in the regenerating fin. The distance is measured from the expression domain (determined by whole mount ISH) to the distal end of the fin, using the third fin ray as a standard, as previously established (Iovine and Johnson, 2000). Irregular (+/-) expression of *evx1*was observed in the *alf*^{dty86} fins, while *dlx5a* and *mmp9* gene expression was present in all fin rays (+).The *evx1*expression domain in the *alf*^{dty86} fins was measured from the subset of *evx1*-positive fin rays. N, number of fins.

3.6 References

Akimenko, M.A., et al., 2003. Old questions, new tools, and some answers to the mystery of fin regeneration. *Dev Dyn* .226: 190-201.

Borday, V., et al., 2001. *evx1* transcription in bony fin rays segment boundaries leads to a reiterated pattern during zebrafish fin development and regeneration. *Dev Dyn* .220: 91-98.

Brown, A.M., et al., 2009. Osteoblast maturation occurs in overlapping proximal-distal compartments during fin regeneration in zebrafish. *Dev Dyn*. 238: 2922-2928.

Faiella, A., et al., 1991. Isolation and mapping of EVX1, a human homeobox gene homologous to even-skipped, localized at the 5' end of HOX1 locus on chromosome 7. *Nucleic Acids Res*. 19: 6541-6545.

Hoptak-Solga, A.D., et al., 2008. Connexin43 (GJA1) is required in the population of dividing cells during fin regeneration. *Dev Biol* .317: 541-548.

Iovine, M.K., et al., 2005. Mutations in *connexin43* (GJA1) perturb bone growth in zebrafish fins. *Dev Biol* .278: 208-219.

Iovine, M.K., Johnson S.L., 2000. Genetic analysis of isometric growth control mechanisms in the zebrafish caudal fin. *Genetics*. 155: 1321-1329.

Knopf, F., et al., 2011. Bone regenerates via dedifferentiation of osteoblasts in the zebrafish fin. *Dev Cell*. 20: 713-724.

Landis, W.J., Geraudie J., 1990. Organization and development of the mineral phase during early ontogenesis of the bony fin rays of the trout Oncorhynchus

mykiss. *Anat Rec*. 228: 383-391.

Lee, Y., et al., 2005. Fgf signaling instructs position-dependent growth rate during zebrafish fin regeneration. *Development*. 132: 5173-5183.

Lee, Y., et al., 2009. Maintenance of blastemal proliferation by functionally diverse epidermis in regenerating zebrafish fins. *Dev Biol*. 331: 270-280.

Mari Beffa, M., et al., 1989. Elastoidin turn over during tail fin regeneration in teleosts. A morphometric and radioautographic study. *Anat Embryol (Berl)*. 180: 465-470.

Pacifici, M., et al., 2006. Cellular and molecular mechanisms of synovial joint and articular cartilage formation. *Ann N Y Acad Sci*. 1068: 74-86.

Poss, K.D., et al., 2003. Tales of regeneration in zebrafish. *Dev Dyn*. 226: 202-210.

Quint, E., et al., 2002. Bone patterning is altered in the regenerating zebrafish caudal fin after ectopic expression of sonic hedgehog and bmp2b or exposure to cyclopamine. *Proc Natl Acad Sci U S A*. 99: 8713-8718.

Santamaria, J.A., et al., 1992. Interactions of the lepidotrichial matrix components during tail fin regeneration in teleosts. *Differentiation*. 49: 143-150.

Schulte, C.J., et al., 2011. Evx1 is required for joint formation in zebrafish fin dermoskeleton. *Dev Dyn*. 240: 1240-1248.

Sims, K., et al., 2009. Connexin43 regulates joint location in zebrafish fins. *Dev Biol*. 327: 410-418.

Singh, S.P., et al., 2012. Regeneration of amputated zebrafish fin rays from de novo osteoblasts. *Dev Cell*. 22: 879-886.

Sousa, S., et al., 2011. Differentiated skeletal cells contribute to blastema formation during zebrafish fin regeneration. *Development*. 138: 3897-3905.

Talbot, J.C., et al., 2010. hand2 and dlx genes specify dorsal, intermediate, and ventral domains within zebrafish pharyngeal arches. *Development*. 137: 2507-2517.

Thummel, R., et al., 2006. Inhibition of zebrafish fin regeneration using in vivo electroporation of morpholinos against *fgfr1* and *msxb*. *Dev Dyn*. 235: 336-346.

Ton, Q.V., Iovine M.K., 2012. Semaphorin3d mediates Cx43-dependent phenotypes during fin regeneration. *Dev Biol*. 366: 195-203.

Tu S., Johnson S.L., 2011. Fate restriction in the growing and regenerating zebrafish fin. *Dev Cell*. 20: 725-732.

van Eeden, F.J., et al., 1996. Genetic analysis of fin formation in the zebrafish, Danio rerio. *Development*. 123: 255-262.

Westerfield, M., 1993. The Zebrafish Book: A guide for the laboratory use of zebrafish (Brachydanio rerio). . Eugene, OR: University of Oregon Press.

Yoshinari, N., et al., 2009. Gene expression and functional analysis of zebrafish larval fin fold regeneration. *Dev Biol*. 325: 71-81.

Chapter 4

Remaining Questions and Future Direction

4.1 Introduction

The focus of my thesis dissertation is defining the relevant Cx43 functions during skeletal morphogenesis to reveal the initial Cx43-dependent event that regulates changes in cellular function, whether Cx43 functions as a gap junction channel, a hemichannel, or in a channel-independent manner. Still, several questions remain open regarding (1) how Cx43 influences gene expression in the lateral skeletal precursor cells, (2) how Cx43 is regulated in turn mediates effects of skeletal patterning. This chapter is an attempt to provide a synopsis of some preliminary work in order to recommend further interests for future inquiry.

4.2 How does Cx43 influence gene expression in the lateral skeletal precursor cells?

It has been established that Cx43-based GJIC contributes to skeletal development but it remains unclear how. Others have shown that in osteoblast-like cell lines changes in the level of Cx43 based GJIC influences the expression of osteoblast genes. This work has been completed using a reporter assay in osteoblast cell lines (i.e., ROS17/2.8 cells and/or MC3T3 cells). The reporter construct contains the promoter of the osteoblast-specific gene osteocalcin upstream of the luciferase coding sequence. Luciferase activity can be precisely calculated and is directly proportional to the level of gene transcription from the osteocalcin promoter. When Cx43 function is high, luciferase activity is high. When Cx43 function is abrogated either by over-expression of Cx45 (which has been shown to reduce Cx43-dependent GJIC by modifying the size and specificity of the heteromeric gap junction channel, Lecanda et al., 1998) or by the addition of pharmacological inhibitors of GJIC (Stains and Civitelli, 2005), luciferase activity is reduced. Using this system, two distinct Cx43-dependent response elements have been identified in the osteocalcin promoter, and a mechanism for Cx43-dependent transcriptional activation has been suggested. In addition, a minimal Cx43 response element (CxRE) was identified in the osteocalcin promoter (Stains et al., 2003). It was determined that Cx43 function regulated the level of phosphorylation of the transcription factor Sp1, which in turn is bound to the CxRE. Thus, increased phosphorylation of Sp1 favored its recruitment to the CxRE and caused increased gene transcription. In contrast, reduced phosphorylation of Sp1 favored the recruitment of an alternate transcription factor, Sp3, and leads to reduced gene transcription. Continued studies revealed that the phosphorylation of Sp1 occurred through Cx43-dependent activation of the ERK signal

transduction cascade (Stains and Civitelli, 2005). Moreover, this Cx43-dependent recruitment of Sp1 was also correlated with recruitment of the osteoblast transcription factor Osx/Sp7 to the osteocalcin promoter (Niger et al., 2011). A second pathway for Cx43-dependent gene transcription occurs via activation of the transcription factor Runx2. Phosphorylated Runx2 interacts with the osteoblast-specific element OSE2, also found in the osteocalcin promoter. Cx43 function leads to activation of PKCδ, which is an intermediate in the FGF2 signaling pathway. Activation of PKCδ leads to the phosphorylation of Runx2 and increased gene transcription (Lima et al., 2009). Alternatively, FGF2 signaling can activate ERK independent of Cx43, also leading to Runx2-phosphorylation (Niger et al., 2012). These data provide evidence that FGF2 and Cx43 synergize to influence Runx2-phosphorylation and therefore increased gene expression of at least a subset of osteoblast-specific genes. How are the ERK and FGF2 growth factor dependent signaling cascades related to Cx43 function? The Stains group suggests that both primary and secondary responses to growth factor-mediated signal transduction pathways are responsible for coordinated regulation of gene expression among a population of osteoblasts. The primary response occurs in cells expressing appropriate receptors for externally provided cues, such as growth factors. Growth factor binding to its receptor leads to the intracellular production of second messengers, which in turn can be shared with adjacent cells via gap junctions, thereby promoting the same response in neighboring cells (i.e., even when those cells lack the appropriate receptor). The identification of signal transduction cascades working synergistically with Cx43-based gap junctions suggests that one role of gap junctions may be to amplify typical growth-factor induced responses. Moreover, as the carboxy-tail of connexins may act as a

signaling center by binding to components of various signaling complexes (Bivi et al.,2011), the mediators of the second messengers may be closely associated with gap junctions. For example, Ras, a mediator of the ERK pathway, is known to associate on the inner leaflet of the plasma membrane and could associate with gap junctions (Stains and Civitelli, 2005). Moreover, PKCδ, a known mediator of FGF2 signaling, was recently shown to physically associate with the carboxy-tail of Cx43 (Niger et al., 2010).

In chapter 2, I provided evidence that Cx43 activity strongly correlated with levels of *sema3d* expression. However, since *sema3d* expression is in a different population of cells, it is uncertain how *cx43* present in the blastema could influence *sema3d* expression in the lateral compartment. I suggest two models to address this question (reviewed in Ton and Iovine, 2013). First, Cx43-GJIC may cause changes in gene expression in the *cx43*-positive compartment that lead to the secretion of an unidentified growth factor. This growth factor may bind to its receptor on the adjacent cells (i.e. skeletal precursor cells) and cause an increase in *sema3d* expression in the lateral compartment (Figure 4.1a). Such a mechanism may be revealed by continued examination of genes identified from the microarray analysis (described in Ton and Iovine, 2012). There is also another possibility that a junctional complex that may regulate *sema3d* transcriptional expression. For example, Cx43 channels could physically bind to tight junction components interacting with transcription factors in the neighboring cell to control downstream gene expression (reviewed in Vinken et al., 2012). If this is the case, we need to investigate which tight junctional complex that can bind to Cx43.

We also need to identify potential transcription factors that could bind to the complex in turn regulate *sema3d*.

For the second model, I propose that heterotypic gap junctions (i.e. when each cell contributes a connexon composed of different connexins) exist between cells of the blastema and the skeletal precursor cells (Figure 4.1b). Our data suggest that the two population of cells in the medial and lateral compartments may use Cx43 based gap junction to communicate with the surrounding environment activating signaling pathways that could alter cell cycle (for growth) and cellular differentiation (for joint). This hypothesis is consistent with the requirement of *smedinx-11* during planarian regeneration (*smedinx* is one type of *connexin* (called *innexin* in planarian) gene (Oviedo and Levin 2007). In our scenario, Cx43 activity in the medial compartment could now directly transmit signals that influence gene expression in the lateral skeletal precursor cells via GJIC. Expression of a *connexin* gene has not been identified in the lateral compartment. However, since the zebrafish genome has at least 37 connexin genes (Eastman et al., 2006), one may still be found. This latter model, if true, may represent an *in vivo* example of second messengers traveling from one cell population to another in order to coordinate changes in gene expression.

4.3 How is Cx43 activity regulated?

Zebrafish joints occur in the intramembraneous ossification (Flores et al., 2004; Kang et al., 2004; Yan et al., 2005), unlike synovial joints which occur in the cartilage/endochondral skeleton (Pacifici et al., 2006). Although mechanisms that regulate joint formation in zebrafish are still largely unknown, studies shows that joint

morphogenesis in chicks and mouse begins with a condensation of a subset of mesenchymal cells (Eames et al., 2003; Pacifici et al., 2006). We identified a similar condensation of mesenchymal cells early in joint development of fin regeneration (Sims et al., 2009). In chapter 3, it was shown that changes in Cx43 activity located in the blastema influence joint gene expression in the lateral skeletal precursor cells. In addition, *cx43*-KD and *plxna3*-KD experiments rescue the irregular pattern of *evx1* expression in *alf* ^{dty86} (chapter 3). Thus, we believe that Cx43 could be the main regulator for joint formation. In addition, Cx43 rescues joints by regulating Sema3d-PlxnA3 signaling to rescue *evx1* expression. Further, our initial data support the hypothesis that Cx43 suppresses joint formation. It follows that *cx43* expression must be reduced to permit joint formation. To test this hypothesis, we first attempted to evaluate joint morphology over time.

Previously, our study shows that the morphology of young versus mature joints can be clearly distinguished (Sims et al., 2009; Figure 4.2). Since the fin grows from a proximal to distal direction, new joint and new tissue can be found in the distal end of the fin. Thus, a young joint is located distally and can be detected as a single row of cells that appears as condensations of ZNS5-positive cells. At this time, bone matrix remains uninterrupted; we refer to this as presumptive joint. Shortly thereafter as joint cells transition to more mature morphology, physical separation of bone matrix occurs. The mature joint appears more proximal as two rows of cells where each row flanks a joint (Figure 4.2). We next examined joint morphology over time (i.e. 48 hpa to 144 hpa). The first young joint appears at 87 hpa in the third fin ray. Mature joints appear by 96 hpa. Next, we attempted to correlate *cx43* expression with joint morphology. We performed

whole mount ISH, cryo ISH, and qRT-PCR to examine this correlation. Indeed, we observed the appearance of first young joint that is correlated with the decreased level of *cx43* gene expression (Figure 4.3; Table 4.1). We thus concluded that transient reduction in *cx43* expression correlated with presumptive joints, supporting our previous hypothesis that Cx43 suppresses joint formation.

From chapter 3, we established an *evx1*-dependent joint pathway (*evx1-dlx5a-mmp9*) that is regulated by Cx43 activity. We next attempted to correlate changes in joint gene expression with the timing of joint formation. We predicted that *evx1* expression will be up-regulated as *cx43* expression gets down-regulated. Indeed, we found that the level of *evx1* expression is up-regulated at 87 hpa (Figure 4.4). Expression of other genes downstream of *evx1* genes (*dlx5a* and *mmp9*) are also correlated with changes in *cx43* expression through time. For example, *dlx5a* expression is expanded at 87 hpa. Interestingly, the level of *mmp9* peaks a bit later at 96 hpa (Figure 4.4). MMP9 is a matrix metalloproteinase (MMP) protein. It is possible that *mmp9* becomes up-regulated later in concert with the formation of physical separation of the bone matrix. Future studies are required to determine if this is the case. Taken together, our final data suggest that Cx43 activity is negatively correlated with the expression of joint markers, especially with *evx1* expression (Figure 4.5). These data provide insights into how joints become premature in *sof*^{b123} and how joints fail in *alf*^{dty86}. Premature joints may occur due to the lower level of *cx43*, which ultimately relieves the inhibition of the *evx1*-dependent joint pathway too early. Joint failure may occur due to the high level of *cx43*, which is rarely reduced sufficiently to relieve the inhibition on *evx1* expression.

It is interesting that while *cx43* mRNA expression has a modest reduction at 87 hpa, the level of Cx43 protein appears little to no different compared with other time line (Figure 4.6). Taken this result into consideration, we wish to explore Cx43 localization through time to locate the position of Cx43 relative to whether it is at either the cytoplasm or at the plasma membrane. Since studies show that gap junction channel is functional once Cx43 assembles at the plasma membrane (Lampe et al., 2000; Jordan et al., 1999), we predict that Cx43 protein could be cytoplasmic at 87 hpa. To test this, we will first examine localization of Cx43 within time course (72 hpa, 87 hpa and 96 hpa) by utilizing transgenic fish; Tg(b-actin:HRAS-EGFP)vu119 that has reporter c-Ha-Ras gene (GTPase) fused to eGFP for plasma membrane visualization (generous gift from Dr. Poss; original construct from Lila Solnica-Krezel lab, Vanderbilt University). Localization of Cx43 at specific time line thus will be determined by using antibodies against Cx43 (red) in the Ras transgenic fish that is used as membrane marker (green). Under the confocal microscope, we will then look for red and green signals whether they are co-localized or separated reflecting whether Cx43 is cytoplasmic or at the membrane.

In addition, we wish to explore the roles of phosphorylation over time. Several studies show direct roles of phosphorylation in connexins that are involved in intracellular communication have different distinct roles (reviewed in Laird 2005). For example, there is abundant evidence showing that phosphorylation events are involved in marking connexin proteins (i.e. Cx43) for degradation thus increasing the rate of turnover (reviewed in Laird 2005). However, other research shows that phosphorylation events do not appear to be a pre-requisite for degradation. For example, study shows Cx43-GFP fused construct appears fully functional at the plasma membrane and is still

phosphorylated within live mammalian cells (Jordan et al., 1999). Further, phosphorylation events through Akt activation rescue the gap junction from potential degradation (Dunn et al., 2012). In MDCK cell line, activation of Akt phosphorylates Cx43 in turn results in gap junction stabilization (Dunn et al., 2012). Perhaps phosphorylation occurring at different residues could lead to different outcomes seen in these studies. Thus, we wish to explore phosphorylation events during the regeneration time course (72 hpa, 87 hpa and 96 hpa) by using phosphor-specific-antibodies against specific residues at the C-terminal of Cx43 that have potential to be phosphorylated. These future studies will provide physical evidence to explain when/where Cx43 based GJIC channels get modified and whether phosphorylation events at different residues occurring at a specific time could be one of the reasons causing the downstream events (i.e. joint inhibition).

My graduate work has focused on defining tangible Cx43-dependent pathways that regulate skeletal morphogenesis. I have revealed the connection between Cx43 and Sema3d signaling pathways that regulate growth and skeletal patterning in fin regeneration. Upstream events that could regulate Cx43 still remain under questions. FGF4 signaling in the developing limb bud has shown to be responsible for cell-cell communication (i.e. Cx43-GJIC in the posterior mesenchyme cells at the tip of the bud) (Makarenkova et al., 1997). Further, FGF signaling is commonly known to contribute to fin regeneration (reviewed in Poss 2010). Thus, we speculate that FGF signaling might function upstream of Cx43 in zebrafish fin regeneration. Moreover, in recent years, several studies have showed evidence of micro RNAs (miRNA) that have potential functions to regulate Cx43. For example, miRNA-206 targets Cx43 to regulate osteoblast

differentiation in primary osteoblast cell lines (Inose et al., 2009). In zebrafish heart regeneration, *cx43* is the target of miR-133 (Yin et al., 2012). Interestingly miR-133 may have an additional role in zebrafish fin regeneration. Study shows that when miR-133 is increased, fin regeneration is attenuated. Fgf signaling can alter miR-133 expression to facilitate cell proliferation in the blastema and tissue renewal (Yin et al., 2008). It is still unknown whether *cx43* is the target in this scenario. In addition, it is reported that more than one micro-RNAs could target several potential genes to directly regulate fin regeneration (Thatcher et al., 2008), suggesting that micro RNAs indeed play essential roles for regeneration. Thus, at least one micro RNA acts upstream of Cx43 and whether or not miR-133 regulates *cx43*-dependent phenotypes remains for us to find.

Most studies in regenerative field focus on pluripotent stem cells *in vitro* as the potential application to replace lost or damaged tissues with new ones. However, to gain a complete understanding of regeneration, researchers must study the processes *in vivo*. Several *in vitro* studies of bone and joint development have demonstrated central roles of Cx43 in skeletal development (Plotkin and Bellido 2013). For example, Cx43 serves as a scaffold regulator for osteoblast survival and its activity (reviewed in Plotkin and Bellido 2013). Cx43 also represents as a mediator for other intercellular signal transduction such as calcium signaling that eventually influences downstream effects (reviewed in Rossello and Kohn 2009). Here, I have revealed the connection between Cx43 and Sema3d signaling pathway that in turn regulates cell proliferation and differentiation for growth and skeletal patterning *in vivo*. Several extensive studies have mainly utilized classical approaches such as conduction, induction and cell transplantation to enhance cell differentiation and tissue regeneration (reviewed in Rossello and Kohn 2009). Recently,

researchers have begun to focus on paracrine signals secreted by different populations of cells. For example, they developed a new strategy by co-culturing vascular endothelial cells with osteoblasts in a three-dimensional system in a silk fibroin scaffold (reviewed in Grellier et al., 2013). They think that if they have a better understanding of biological processes underlying cell-cell communication between these two populations, they would be able to improve vascularization in a bone substitute to enhance the survival of cells. They also think that with this strategy live grafts will not only substitute when implanted but can repair defected bone, providing a good implication to vascular bone tissue engineering. In our scenario, we hope that once we understand how Cx43 is regulated, what regulates Cx43, and how communication is achieved between the two populations of cells (i.e. the medial compartment and the lateral compartment), it might present some new knowledge in regeneration in addition to new strategies for the bone tissue engineering.

4.4 Figures

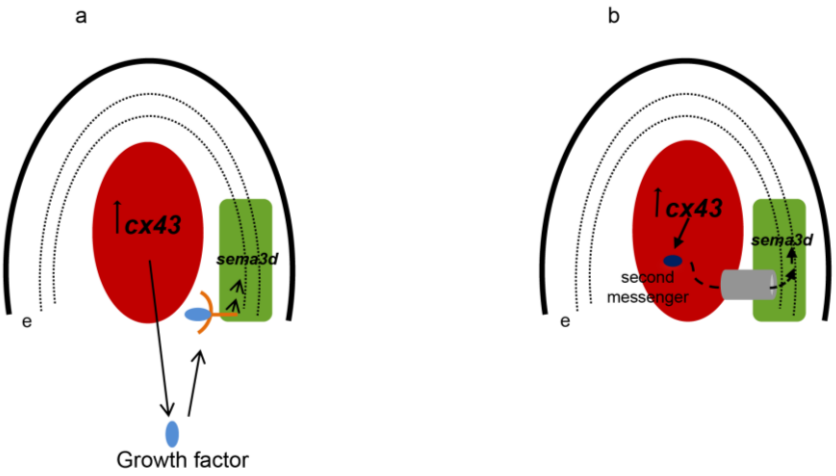

Figure 4.1 Examples of how Cx43-dependent GJIC may influence gene expression in the regenerating fin. (a) Up-regulation of *cx43* in the blastema (red) may lead to the secretion of a growth factor that can interact with its receptor located on adjacent skeletal precursor cells (green), leading to increased *sema3d* expression. (b) Heterotypic gap junctions may exist between cells of the blastema and skeletal precursor cells, permitting the direct exchange of secondary messengers. These second messengers may influence *sema3d* expression. Reviewed in Ton and Iovine, 2013.

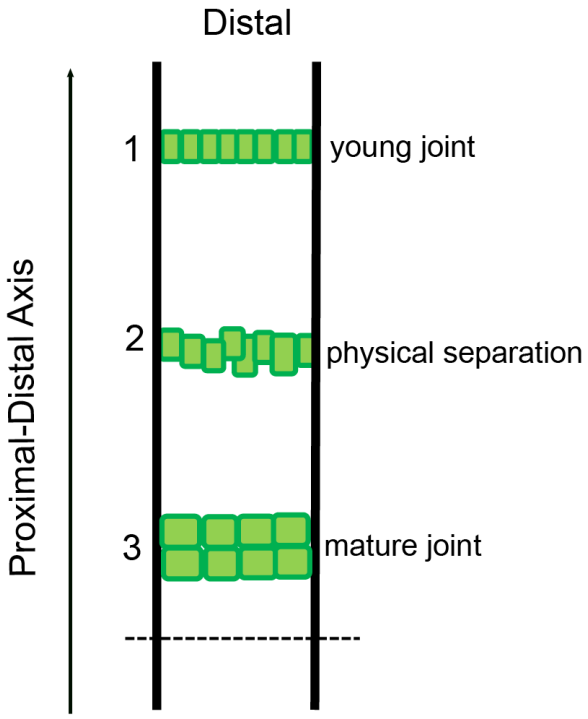

Figure 4.2: Joint morphology in zebrafish fin rays. Cartoon depicts joint morphology at 5 dpa. The youngest (newest) joint (joint 1) is located distally, seen as a single row of cells. Fins grow in a proximal-distal axis as joints become more mature. Mature joint (joint 3) appears under two rows of cells.

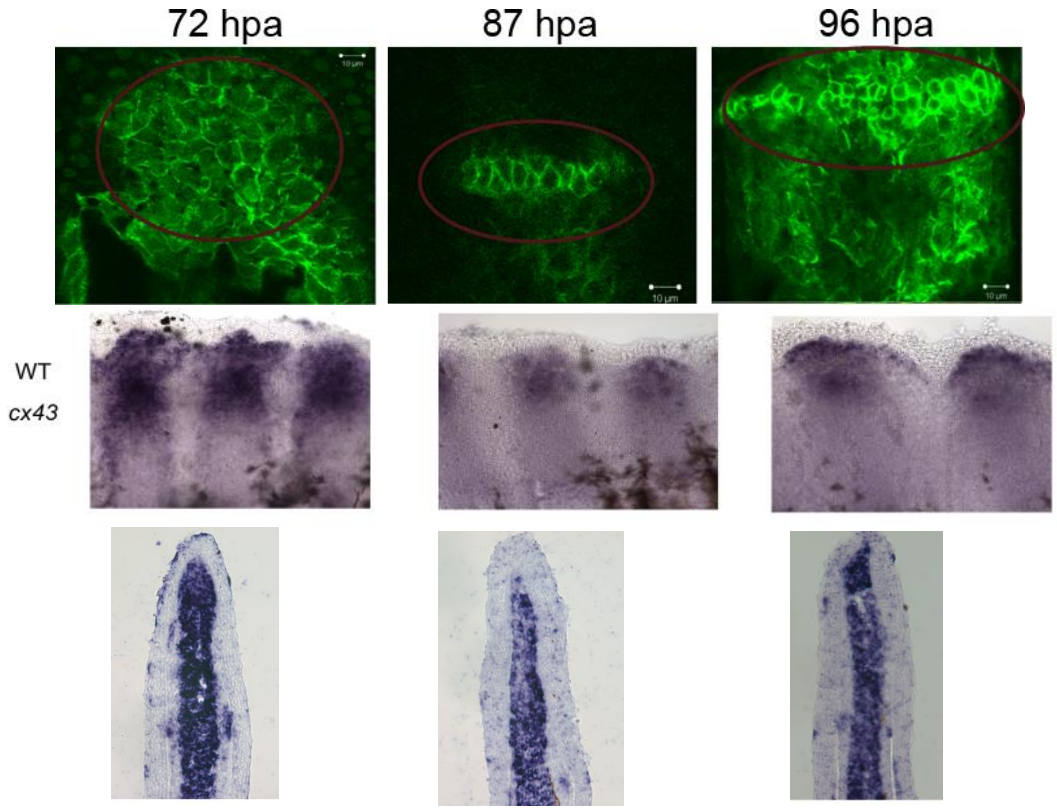

Figure 4.3: First young joint is detected when *cx43* is down-regulated. Upper panel: First joint is detected at 87 hpa. Middle panel: Whole mount in situ hybridization (ISH) shows *cx43* down-regulated at 87 hpa. Bottom panel: In situ hybridization (ISH) on cry-sections show *cx43* expression reduced in the mesenchymal compartment.

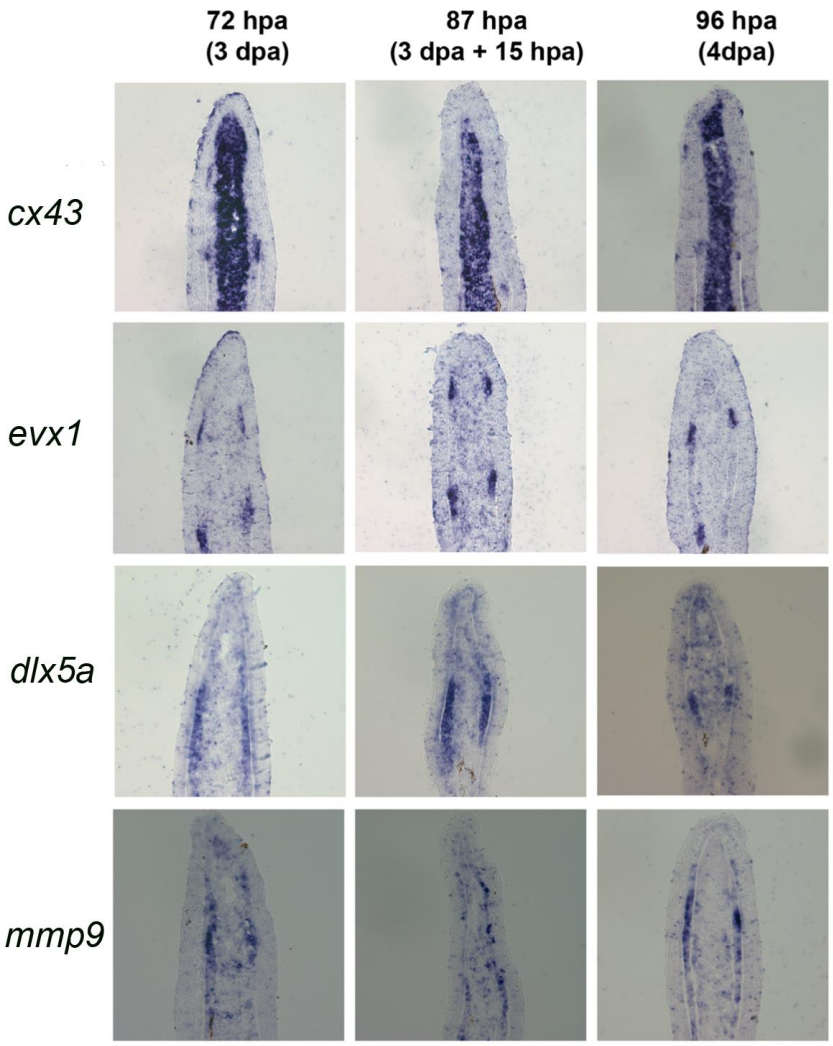

Figure 4.4: Expression of joint gene markers are coordinated with Cx43 activity. In situ hybridization (ISH) on cryo-sections shows up-regulation in *evx1* expression and the expansion of *dlx5a* expression at 87 hpa, while *cx43* expression is downregulated. The expression of *mmp9* is slightly higher at 96 hpa since it is required for the physical separation of joint cells when they start to mature. Whole mount ISH also shows this correlation of the joint markers with *cx43* expression (Data not shown).

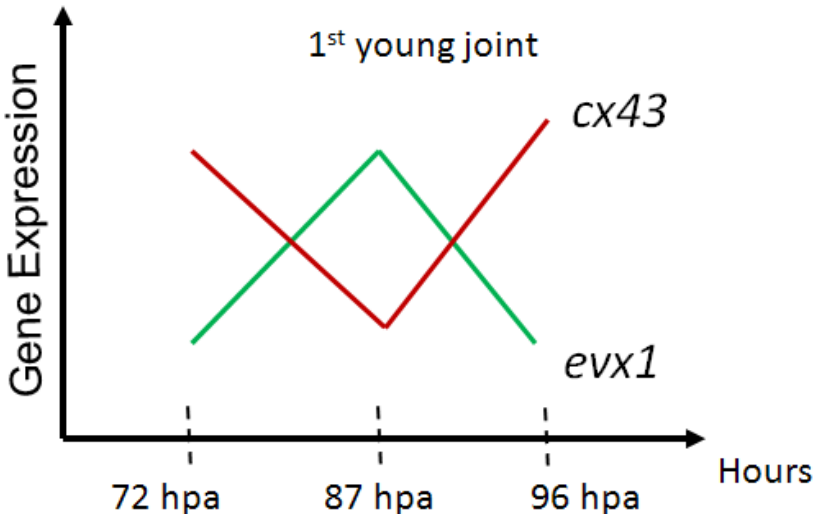

Figure 4.5: Cx43 activity negatively corelated with *evx1* expression. Graph shows when first young joint is detected at 87 hpa, *cx43* expression is down-regulated while *evx1* expression becomes up-regulated, confirming our hypothesis that Cx43 suppresses joint formation.

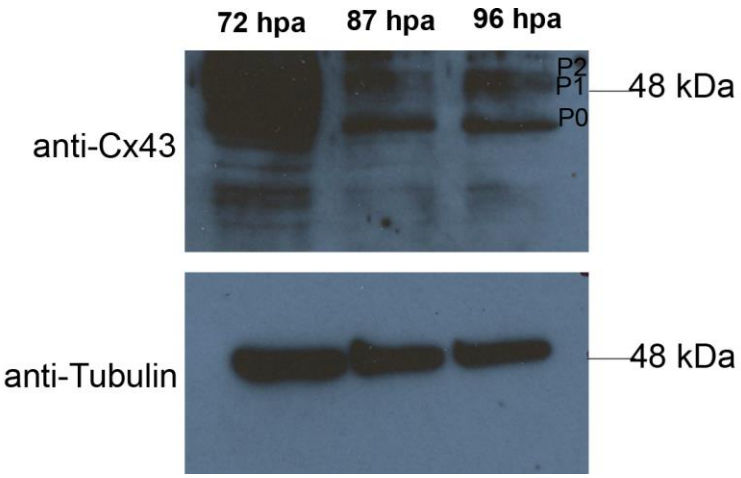

Figure 4.6: Level of Cx43 protein is slightly reduced at 87 hpa. Western blot shows different level of Cx43 protein through time. Cx43 has 3 phosphorylation sites P0, P1, and P2. Tubulin was used for control.

	72 hpa	87 hpa	96 hpa
ΔC_t (C_t *cx43* - C_t *ker4*)	3.27 2.89 3.16	5.41 4.49 4.24	4.23 3.39 3.98

High ΔC_t values indicate low gene expression

Table 4.1: *cx43* is normally down-regulated at time of joint initiation. qRT-PCR shows ΔC_t of *cx43* at 87 hpa is one to two cycles later compared with 72 hpa and 96 hpa.

4.5 References

Bivi, N., et al., 2011. Connexin43 interacts with βarrestin: a prerequisite for osteoblast survival induced by parathyroid hormone. *J Cell Biochem*. 112: 2920-2930.

Dunn, C. A., et al., 2012. Activation of Akt, not Connexin 43 protein ubiquitination, regulates gap junction stability. *J Biol Chem*. 287**,** 2600-7.

Eastman, S. D., et al., 2006. Phylogenetic analysis of three complete gap junction gene families reveals lineage-specific duplications and highly supported gene classes. *Genomics*. 87**,** 265-74.

Eames, B.F., et al., 2003. Molecular ontogeny of the skeleton. *Birth Defects Res. C. Embryo Today*. 69, 93-101.

Flores, M.V., et al., 2004. Duplicate zebrafish runx2 orthologues are expressed in developing skeletal elements. *Gene Expr. Patterns*. 4, 573-581.

Grellier, M., et al., 2013. Cell-to-cell communication between osteogenic and endothelial lineages: implications for tissue engineering. *Trends in Biotechnology*. 27, 562-571.

Inose, H., et al., 2009. A microRNA regulatory mechanism of osteoblast differentiation. *Proc Natl Acad Sci U S A*. 106**,** 20794-9.

Jordan, K., et al., 1999. Trafficking, assembly, and function of a connexin43-green fluorescent protein chimera in live mammalian cells. *Mol Biol Cell*. 10**,** 2033-50.

Laird, D. W., 2005. Connexin phosphorylation as a regulatory event linked to gap junction internalization and degradation. *Biochem Biophys Acta*. 1711**,** 172-82.

Kang, J.S., et al., 2004. Characterization of dermacan, a novel zebrafish lectican gene, expressed in dermal bones. *Mech. Dev.* 121, 301-312.

Rossello, R.A. and Kohn D.H. 2009. Gap junction intercellular communication: A review of a potential platform to modulate craniofacial tissue engineering. *J Biomed Mater Res B Appli Biomater*. 88(2): 509-518.

Lampe, P. D., Lau, A. F., 2000. Regulation of gap junctions by phosphorylation of connexins. *Arch Biochem Biophys*. 384**,** 205-15.

Lecanda, D., et al., 1998. Gap junctional communication modulates gene expression in osteoblastic cells. *Mol Biol Cel*l. 9: 2249-2258.

Lima, F., et al., 2009. Connexin43 potentiates osteoblast responsiveness to fibroblast growth factor 2 via a protein kinase C-delta/Runx2-dependent mechanism. *Mol Biol Cell*. 20**,** 2697-708.

Makarenkova, H., et al., 1997. Fibroblast growth factor 4 directs gap junction expression in the mesenchyme of the vertebrate limb bud. *J Cell Biol*. 138(5): 1125-1137.

Niger, C., et al., 2010. Interaction of connexin43 and protein kinase C-delta during FGF2 signaling. *BMC Biochem*. 11:14

Niger, C., et al., 2011. The transcriptional activity of osterix requires the recruitment of Sp1 to the osteocalcin proximal promoter. *Bone*. 49: 683-692.

Niger, C., et al., 2012. ERK acts in parallel to PKCdelta to mediate the *connexin43*-dependent potentiation of Runx2 activity by FGF2 in MC3T3 osteoblasts. *Am J Physiol Cell Physiol*. 302**,** C1035-44.

Niger, C., et al., 2011. The transcriptional activity of osterix requires the recruitment of Sp1 to the osteocalcin proximal promoter. *Bone*. 49**,** 683-92.

Oviedo, N.J. and Levin M. 2007. smedinx-11 is a planarian stem cell gap junction gene required for regeneration and homeostasis. *Development*. 134 (17): 3121-31.

Pacifici, M., et al., 2006. Cellular and molecular mechanisms of synovial joint and articular cartilage formation. *Ann N Y Acad Sci*. 1068:74-86.

Plotkin L.I. and Bellido T. 2013. Beyond gap junctions: Connexin43 and bone cell signaling. *Bone*. 1, 157-166.

Poss, K.D. 2010. Advances in understanding tissue regenerative capacity and mechanisms in animals. *Nature Review Genetics*. 11, 710-722.

Sims, K., Jr., et al., 2009. Connexin43 regulates joint location in zebrafish fins. *Dev Biol*. 327**,** 410-8.

Stains, J.P., et al., 2003. Gap junctional communication modulates gene transcription by altering the recruitment of Sp1 and Sp3 to connexin-response elements in osteoblast promoters. *J Biol Chem*. 278: 24377-24387.

Stains, J. P., Civitelli, R., 2005. Cell-cell interactions in regulating osteogenesis and osteoblast function. *Birth Defects Res C Embryo Today*. 75**,** 72-80.

Thatcher, E. J., et al., 2008. Regulation of zebrafish fin regeneration by microRNAs. *Proc Natl Acad Sci U S A*. 105**,** 18384-9.

Ton, Q. V., Iovine, M. K., 2013. Determining how defects in Connexin43 cause skeletal disease. *Genesis*. 51**,** 75-82.

Ton, Q. V., Kathryn Iovine, M., 2012. Semaphorin3d mediates Cx43-dependent phenotypes during fin regeneration. *Dev Biol*. 366**,** 195-203.

Vinken, M., et al., 2012. Non-channel functions of connexins in cell growth and cell death. *BBA-Biomembranes*. 8, 2002-2008.

Yan, Y.L., et al., 2005. A pair of Sox: distinct and overlapping functions of zebrafish sox9 co-orthologs in craniofacial and pectoral fin development. *Development*. 132, 1069-1083.

Yin, V. P., et al., 2012. Regulation of zebrafish heart regeneration by miR-133. *Dev Biol*. 365**,** 319-27.

Yin, V. P., et al., 2008. Fgf-dependent depletion of microRNA-133 promotes appendage regeneration in zebrafish. *Genes Dev*. 22**,** 728-33.

Conclusions

Research from the Iovine lab has suggested that Cx43 coordinates cell proliferation with joint formation. Using genetics approach and functional test (i.e. morpholino mediated gene knockdown), I have identified a major signaling pathway, Sema3d, that acts downstream of *cx43* mediating *cx43*- dependent phenotypes. Data also elucidates an *evx1*-dependent joint pathway that acts and mediated by Cx43-Sema3d-Plxna3 signaling. Further, Cx43 activity appears correlated with joint gene expression that ultimately permits joint formation. Overall, this dissertation has contributed to a better understanding about the influence of Cx43 based gap junctional activity on semaphorin signaling leading to downstream effects such as skeletal growth and patterning. Both connexins and semaphorins are widely expressed in human tissues. In addition, semaphorins have been become a drug target since they are showed to be key players in many human pathologies. Thus the coordination between connexins and semaphorins during skeletal morphogenesis should be explored further to provide novel understanding of mechanistic pathways required during skeletal morphogenesis.

QUYNH TON

Curriculum Vitae
Lehigh University Biological Sciences, Iacocca Hall 111 Research Drive
Bethlehem, PA 18015
484-767-6682 · qvt208@lehigh.edu

Education:

Lehigh University, Bethlehem, PA
PhD., Molecular/Cellular Biology, January/2014
Doctoral Thesis: "Determining How Defects In Connexin 43 Cause Skeletal Disease"

Advisor: Dr. Mary Kathryn Iovine

- Identified *semaphorin3d* (*sema3d*) downstream of Connexin43 (Cx43) mediating *cx43*-dependent phenotypes: promoting cell division and suppressing joint formation.
- Defined the joint pathway in fin regeneration.
- Determining joint patterning by characterizing the coordinating event between the level of *cx43* gene expression and the gene expression in the skeletal cells.

Bard College, Annandale-on-Hudson, NY
B.S., Biology, May/2008
Undergraduate Thesis: "Characterization of The Protein Product of Mycobacterium tuberculosis Gene *Rv1373*, A Possible Modulator of The Human Immune Response"

Advisor: Dr. John Ferguson

- Characterized the enzyme specificity of Rv1373 with dehydroepiandrosterone (DHEA), estrone, and estradiol as its substrates.

Volunteer Project: "Exploring *icd1* in Tetrahymena pyriformis for Building Phylogeny Tree"

Advisor: Dr. John Ferguson

- Built a phylogeny tree to compare the conservation of *icd1* throughout species.

Other Project: "Examining Expression Patterns of NR1Ch5 in Zebrafish"

Advisor: Dr. Valeri Thomson

- Examined temporal and spatial expression patterns of NR1Ch5 throughout the development of the zebrafish.

North Shore Community College, Danvers, MA
A.S., Health Sciences, May/2004

Awards:

- Nemes Award Recipient (The award to recognize exceptional students who have demonstrated excellence in research and have made significant progress toward their Ph.D) Fall 2012 (Lehigh University)
- Research and Teaching Assistantships (Lehigh University)
- Recognition for contribution to the Exhibition of Student Research and Scholarship. The 2011 Academic Symposium (Lehigh University)
- Distinguished Science Scholarship (Bard College)
- Bursar's Special Scholarship (Bard College)
- Alumni Scholarship (North Shore Community College)

Laboratory Skills:

- *In situ hybridization* on whole mount and on caudal fin tissue sections.
- Immunofluorescent antibody staining.
- Confocal microscopic imaging.
- Molecular biology and biochemistry techniques (PCR, qRT-PCR, DNA cloning, genotyping, SDS-PAGE, Western blot, bacterial cell lysate, Bradford assay, column chromatography for protein purification, Sulfotransferase activity assay, ELISA).
- Creating and caring for transgenic zebrafish.
- Microinjection techniques.
- Cryo-sectioning of caudal fins.
- Cell culturing and transfection techniques.

Other Skills:

- Phylogeny Analysis software, Chromas, ApE.exe.
- SigmaPlot 9.0, ChemBio Draw Ultra 11.0.
- Adobe Illustrator/Photoshop.
- Microsoft Office (Word, Excel, Power Point).
- Fluency in English and Vietnamese.

Graduate Teaching Experiences:

- Bio Core I: Basis in Molecular/Cellular Biology (01/2012)
- Biochemistry 1 (09/2011)
- Biochemistry Lab (09/2010)
- Bio Core I: Basis in Molecular/Cellular Biology (09/2008)

Publications:

1. **Ton Q.V.** and M. Kathryn Iovine. "Identification of an *evx1*-dependent joint pathway during fin regeneration." *PlosOne* (in revision).
2. **Ton Q.V.** and M. Kathryn Iovine. "Semaphorin3d Mediates Cx43-Dependent Phenotypes During Fin Regeneration." *Developmental Biology*, Volume 366, issue 2 (June 15, 2012), p. 195-203.

3. Cassimeris, L., V. Silva, E. Miller, **Q. Ton**, C. Molnar, J. Fong. "Fueled by microtubles: Does tubulin dimmer/polymer partitioning regulate intracellular metabolism?" *Cytoskeleton*, Volume 69, issue 3 (March 5, 2012), p. 133-143.

Invited Review Publication:

Ton, Q. V. and Iovine, M. K. "Determining How Defects In Connexin43 Cause Skeletal Disease." *Genesis, The Journal of Genetics and Development*, doi: 10.1002/dvg.22349 (2013). Volume 51, (2013), p. 75-82. Figure 4 was selected for the cover image of the Genesis journal Feb 2013.

Oral and Poster Presentations:

1. **Ton Q.** and M. Kathryn Iovine. (2013) "Defining the Joint Pathway in Fin Regeneration." SDB Mid-Atlantic Meeting. College of William and Mary, VA. Poster Award Recipient (The award to recognize the best poster presenters).
2. **Ton Q.** and M. Kathryn Iovine. (2012) "Semaphorin3d Mediates Cx43-Dependent Phenotypes During Fin Regeneration." SDB Mid-Atlantic Meeting. Penn Sate University, PA. *Oral Presenter:* Quynh Ton.
3. **Ton Q.** and M. Kathryn Iovine. (2012) "Semaphorin3d Mediates Cx43-Dependent Phenotypes During Fin Regeneration." 10th International Meeting on Zebrafish Development and Genetics. Madison, WI.
4. **Ton Q.** and M. Kathryn Iovine. (2010) "Characterization of Connexin43 in Joint Development.**"** 9th International Meeting on Zebrafish Development and Genetics. Madison, WI.
5. **Ton Q.** and John Ferguson (2008) "Characterization of The Protein Product of *Mycobacterium tuberculosis* Gene *Rv1373*, A Possible Modulator of The Human Immune Response." Senior Project Conference. Bard College, Annandale-on-Hudson, NY.
6. Choi, Y., E. Cole, J. Dev, N. Gu, X. He, E. Krantz, E. Petras, A. Rahman, **Q. Ton**, W. Wylie, Y. Xiao, J. Zhang, J. Zhou, and V. Thomson (2007) "Examining Expression Patterns of NR1Ch5 in Zebrafish**.**" Hudson Valley Meeting. Annandale-on-Hudson, NY.

Service:

Representative of Biology Organization of Graduate Students (BOGS) for Lehigh University Graduate Senate Student (GSS): participate in Graduate Senate meetings to discuss policies relevant to graduate student life, September 2012- May 2013.

References:

Dr. Mary Kathryn Iovine, Associate Professor, Graduate Coordinator, Lehigh University
Email: mki3@lehigh.edu Phone: 610-758-6981
Dr. Lynn Cassimeris, Professor, Lehigh University
Email: lc07@lehigh.edu Phone: 610-758-6275
Dr. Matthias Falk, Associate Professor, Lehigh University
Email: mfalk@lehigh.edu Phone: 610-758-5896